Enzymatically Triggered Delivery of Proteins from Gel Biomaterials using Orthogonal Sortases

Fariha Rabeya Rahman

A thesis

submitted in partial fulfillment of the

requirements for the degree of

Master of Science in Bioengineering

University of Washington

2020

Committee:

Cole A. DeForest

Kelly Stevens

Program Authorized to Offer Degree:

Bioengineering

University of Washington

Abstract

Enzymatically Triggered Delivery of Proteins from Gel Biomaterials using Orthogonal Sortases

Fariha Rabeya Rahman

Chair of the Supervisory Committee:
Assistant Professor Cole A. DeForest
Departments of Chemical Engineering and Bioengineering

Hydrogel biomaterials have proven useful in a variety of medical and basic life science applications, including as platforms for 3D cell culture and controlled drug delivery. User-defined specification over protein presentation within such gels represents an exciting manner to tune their biochemical properties and their downstream biological effects. Building upon click-polymerized poly(ethylene glycol)-based gels reported previously by our group, this work first demonstrates the application of evolved sortases to site-specifically modify full-length proteins with reactive handles for immobilization within biomaterials, and then to exogenously trigger protein release via orthogonal transpeptidase-catalyzed reactions. This strategy proves effective in dynamically controlling biochemical aspects of gel systems, providing exciting opportunities to model complex physiological processes *in vitro*.

TABLE OF CONTENTS

LIST OF FIGURES

Chapter 1. INTRODUCTION

Biomaterials play a critical role in fields with promising medical applications, such as tissue engineering and drug delivery.[1] Hydrogels, water-swollen polymeric networks, constitute a highly versatile subclass of biomaterials. They can be formulated from a variety of precursors. Components range between complex natural materials (e.g., fibrin, collagen, hyaluronic acid, decellularized extracellular matrix) and broadly modifiable synthetic materials [such as poly(ethylene glycol) and poly(lactic acid)].[2] Hydrogels are attractive engineering targets due to their natural presence in the human extracellular matrix (e.g., hyaluronic acid, fibrin). Additionally, they have highly tunable properties, which enables mimicry of an equally wide range of tissue functions.[2,3] Many of these characteristics fall under the categories of mechanics (e.g., elasticity, porosity, crosslinking density), chemistry (polarity, reactivity), and biochemical composition (e.g., signaling molecule presentation, drug release kinetics).[3]

Crosslinking chemistry is a critical element of hydrogel design for biological applications.[4] Major considerations include selectivity, efficiency, reaction rate, stability of reactants and products, and biocompatibility.[6–8] Common and early crosslinking strategies include radical chain polymerization of (meth)acrylates, enzyme-catalyzed bond formation (e.g., with transglutaminase), and noncovalent guest-host interactions.[5] However, newer strategies involving rapid and catalyst-free click chemistry have further improved the potential biocompatibility of hydrogels and their gelation kinetics, both of which have important consequences for clinical translation. One such strategy is the strain-promoted azide-alkyne cycloaddition (SPAAC, Figure 1.1), which excels in both regards.[9] A strained cyclooctyne ring enables stable conjugation to azide-functionalized molecules at physiological conditions, with high selectivity and no

byproducts.[10] SPAAC has been successfully applied as a crosslinking strategy for poly(ethylene glycol) (PEG)[11] and hyaluronic acid.[12] Other click chemistry strategies have also been applied to crosslinking hydrogels, such as norbornene-tetrazine interactions[13] or Diels-Alder reactions[14].

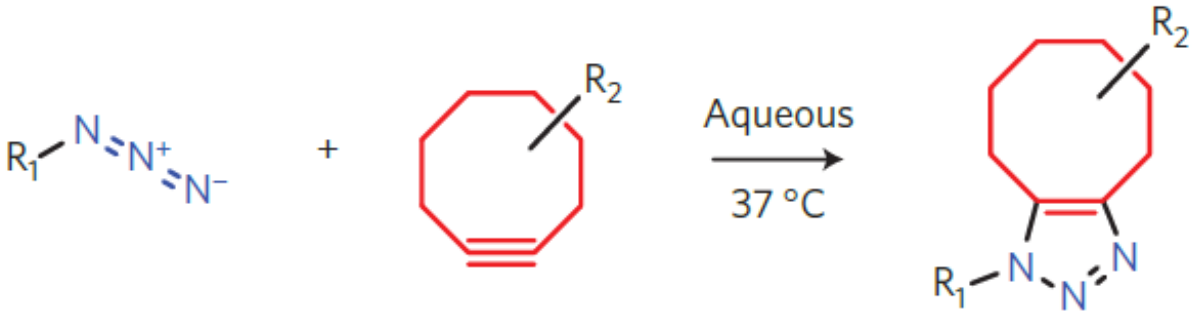

Figure 1.1. Strain-promoted azide-alkyne cycloaddition.[15]

While biocompatible crosslinking impacts both biochemical and mechanical properties of hydrogels, functionalization of biomaterials with biological cues is also a related (and sometimes intertwined) goal for recapitulation of the biochemical complexity found in the highly heterogenous extracellular matrix (ECM).[16] More specifically, there is great interest in developing hydrogel modification strategies to present well-defined and tunable biochemical cues within material environments for *in vitro* models of biological tissue; PEG is especially promising for this purpose.[16–19] PEG has long been modified for user-controlled biochemical cue presentation, such as through the incorporation of photochemistry to mask functional groups.[20] On-demand PEG modification has been successfully applied to models of mesenchymal stem cell (MSC) invasion[21], directing MSC differentiation[15], and potential drug screening platforms[22].

Many enzymes have been applied to site-specifically modifying hydrogels, using their respective peptide substrates, albeit with mechanism-specific limitations. Notably, most enzymes have unidirectional activity, such as cleaving a sequence or catalyzing bond formation irreversibly. However, the *Staphylococcus aureus* sortase A enzyme (SrtA) is a bacterial transpeptidase

involved in modifying cell walls with unusual transpeptidation activity.[23] While its activity falls under the broad umbrella of ping-pong mechanisms by cleaving a short donor substrate sequence (an LPXTG motif) near the C-terminus and forming a tetrahedral intermediate to react with the amine group of a second substrate[24], the completion of the full transpeptidation pathway regenerates the donor substrate[25] (Figure 1.2. *Staph. aureus* sortase A catalytic mechanism.[26]). Thus, a variety of substrates can be recombined or cleaved, and SrtA has consequently been adapted to a wide range of non-native functions.

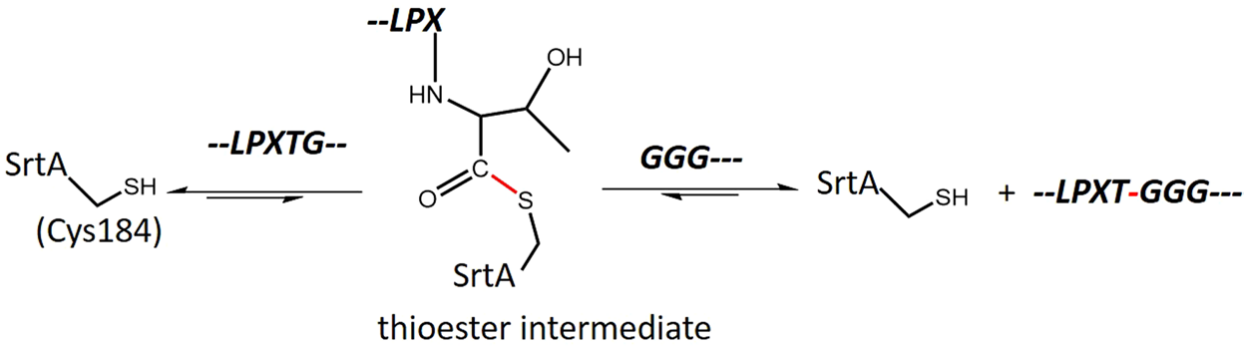

Figure 1.2. *Staph. aureus* sortase A catalytic mechanism.[26]

Wildtype and evolved variants of SrtA have been commonly applied to site-specific modification of proteins for applications in bioconjugation and other biotechnological applications (Figure 1.3).[27–29] Such strategies are typically applied in aqueous conditions, although SrtA has also been useful for modulating hydrogel properties. Site-specific modification of full-length proteins by SrtA has been employed to selectively functionalize proteins with an azide handle, while preserving bioactivity, for SPAAC conjugation to PEG-based gels by this group.[30] To a lesser extent, variants of SrtA have also been used to trigger protein immobilization and release from hydrogels[31–33] and control hydrogel degradation kinetics[34]. They are especially appealing for the rarity of corresponding substrate sequences in the human proteome.[35]

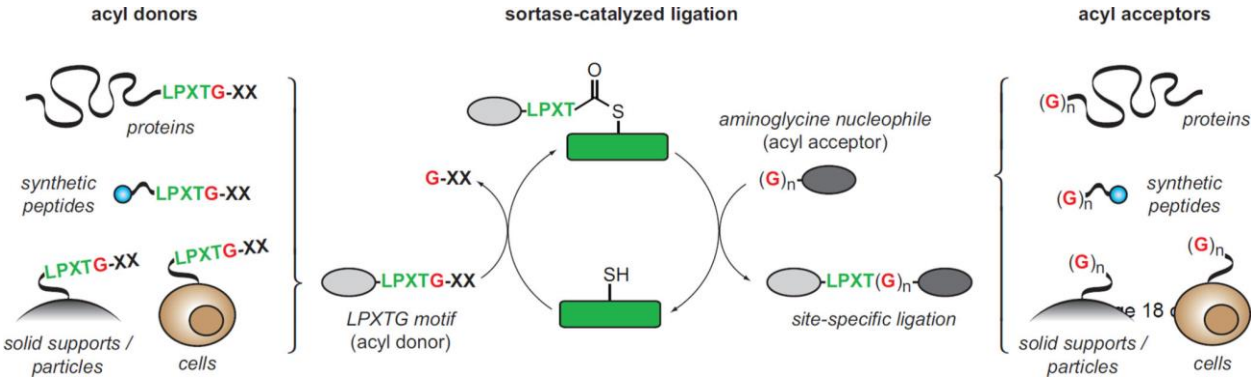

Figure 1.3. Sortase-catalyzed ligation for biotechnological applications.[36]

While other sortases have some substrate diversity, few are as catalytically efficient, and thus as useful outside of their natural context, as SrtA has proven to be in biotechnological applications.[35] Catalytic turnover and the range of available substrates for SrtA has been improved with directed evolution, among a few other strategies.[35,37] The resulting evolved sortases (eSrtAs) have successfully been used to reversibly functionalize surfaces[25] and hydrogels[31–33] individually. Additional evolved variants of the highly catalytically efficient but calcium-dependent eSrtA (5M), which is primarily active against the LPXTG sorting signal, have been developed for activity upon novel sorting signals LAXTG (eSrtA 2A-9) and LPXSG (eSrtA 4S-9).[35] Furthermore, 2A-9 and 4S-9 were co-evolved for relative orthogonality of enzymatic activity, i.e., relatively low cross-reactivity of 2A-9 for the 4S-9 sorting signal (LPXSG) and vice versa.[35] Our group has previously utilized this for orthogonal control over hydrogel degradation.[38]

Here, we exploit eSrtAs 2A-9 and 4S-9 to both modify full-length proteins for immobilization within PEG-based hydrogels and then trigger their orthogonal release from biomaterials. Well-defined hydrogel matrices hold potential for advancing the functionality of engineered tissue constructs and implanted devices.[39–41] More generally, strategies for direct control of matrix properties enable mimicry of the dynamic properties of natural ECM.[3]

Components of this system were selected for bioorthogonality (both in crosslinking and protein immobilization) and flexibility in application, compatible with patterning of short peptides or full-length proteins. The proposed strategy for orthogonal release of full-length proteins could be applied to investigate a variety of biological phenomena, such as modeling dynamic signaling gradients observed in early mammalian development or screening novel drug candidates in more physiologically relevant circumstances through 3D *in vitro* models.

Chapter 2. MATERIALS AND METHODS

2.1 PLASMID CONSTRUCTION

2.1.1 *Sources of initial plasmids*

An existing mRuby-6xHis-encoding pET21 plasmid (backbone from Novagen) and mCerulean-encoding pCMV donated by Daniel Strongin (Fred Hutchinson Cancer Research Center) were subcloned and mutagenized to produce sorting signal-containing fluorescent proteins for downstream azide functionalization.

2.1.2 *Construction of mRuby-LAETG-6xHis-encoding plasmid*

The pET21 plasmid for the original construct, encoding mRuby-6xHis, was used to transform Top10 *Escherichia coli* (*E. coli)* and isolated by Qiaquick mini prep from a 37 °C 5 mL overnight Lysogeny Broth (LB) culture with 0.1 mg/mL carbenicillin. Inverse PCR amplification was used to incorporate the LAETG sorting signal (codon-optimized). The Gibson Assembly method (New England Biosciences, NEB) was used to ligate the ends of the linear mutagenized DNA (1 hour, 37 °C). Gibson Assembly reaction products were used to transform Top10 cells, then plated on carbenicillin selection lysogeny agar (LA) plates. Surviving colonies were used to inoculate 5 mL overnight cultures in LB (carbenicillin 0.1 mg/mL); plasmid DNA was extracted and purified with the QIAgen spin column mini prep kit. Sequencing with a T7 promoter forward primer by Genewiz and alignment by MAFFT in Benchling confirmed expected sequence identity over the full length of the insert.

The open reading frame (5’ → 3’) corresponding to mRuby-LAETG-6xHis is the following:

ATGGTTTCTAAAGGTGAAGAACTGATCAAAGAAAACATGCGTATGAAAGTTGTTATGGAAGGTT

CTGTTAACGGTCACCAGTTCAAATGCACCGGTGAAGGTGAAGGTCGTCCGTACGAAGGTGTTCA

GACCATGCGTATCAAAGTTATCGAAGGTGGTCCGCTGCCGTTCGCTTTCGACATCCTGGCTACC

TCTTTCATGTACGGTTCTCGTACCTTCATCAAATACCCGGCTGACATCCCGGACTTCTTCAAAC

AGTCTTTCCCGGAAGGTTTCACCTGGGAACGTGTTACCCGTTACGAAGACGGTGGTGTTGTTAC

CGTTACCCAGGACACCTCTCTGGAAGACGGTGAACTGGTTTACAACGTTAAAGTTCGTGGTGTT

AACTTCCCGTCTAACGGTCCGGTTATGCAGAAAAAAACCAAAGGTTGGGAACCGAACACCGAAA

TGATGTACCCGGCTGACGGTGGTCTGCGTGGTTACACCGACATCGCTCTGAAAGTTGACGGTGG

TGGTCACCTGCACTGCAACTTCGTTACCACCTACCGTTCTAAAAAAACCGTTGGTAACATCAAA

ATGCCGGGTGTTCACGCTGTTGACCACCGTCTGGAACGTATCGAAGAATCTGACAACGAAACCT

ACGTTGTTCAGCGTGAAGTTGCTGTTGCTAAATACTCTAACCTGGGTGGTGGTATGGACGAACT

GTACAAACTGGCTGAAACCGGTAAGCTTGGTACCCTCGAGcaccaccaccaccaccactga

2.1.3 *Construction of mCerulean-LPESG-6xHis-encoding plasmid*

The sequence for mCerulean was amplified by PCR from a pCMV plasmid. A linear pET21 backbone was inversely amplified from the existing pET21 mRuby-6xHis construct, with incorporation of the LPESG sorting signal (codon-optimized) such that it would fall between mCerulean and the hexahistidine tag in the final construct. PCR reaction products were DpnI digested to remove parent plasmid and purified after agarose gel electrophoresis with the QIAquick gel extraction kit. They were then digested with NdeI and HindIII-HF (NEB), again separated and extracted from agarose gels, and ligated overnight at 16 °C with T4 DNA Ligase (NEB) and a 1:5 ratio of backbone:insert. Ligation mixtures were used to transform Top10 cells, then plated on carbenicillin selection LA plates. Surviving colonies were sequenced with a T7 terminal reverse primer by Genewiz and aligned by MAFFT in Benchling, confirming expected sequence identity over the full length of the insert.

The open reading frame (5’ → 3’) corresponding to mCerulean-LPESG-6xHis is the following:

ATGGTGAGCAAGGGCGAGGAGCTGTTCACCGGGGTGGTGCCCATCCTGGTCGAGCTGGACGGCG

ACGTAAACGGCCACAAGTTCAGCGTGTCCGGCGAGGGCGAGGGCGATGCCACCTACGGCAAGCT

GACCCTGAAGTTCATCTGCACCACCGGCAAGCTGCCCGTGCCCTGGCCCACCCTCGTGACCACC

CTGACCTGGGGCGTGCAGTGCTTCGCCCGCTACCCCGACCACATGAAGCAGCACGACTTCTTCA

AGTCCGCCATGCCCGAAGGCTACGTCCAGGAGCGCACCATCTTCTTCAAGGACGACGGCAACTA

CAAGACCCGCGCCGAGGTGAAGTTCGAGGGCGACACCCTGGTGAACCGCATCGAGCTGAAGGGC

ATCGACTTCAAGGAGGACGGCAACATCCTGGGGCACAAGCTGGAGTACAACGCCATCAGCGACA

ACGTCTATATCACCGCCGACAAGCAGAAGAACGGCATCAAGGCCAACTTCAAGATCCGCCACAA

CATCGAGGACGGCAGCGTGCAGCTCGCCGACCACTACCAGCAGAACACCCCCATCGGCGACGGC

CCCGTGCTGCTGCCCGACAACCACTACCTGAGCACCCAGTCCAAGCTGAGCAAAGACCCCAACG

AGAAGCGCGATCACATGGTCCTGCTGGAGTTCGTGACCGCCGCCGGGATCACTCTCGGCATGGA

CGAGCTGTACAAGCTGCCGGAATCTGGTAAGCTTGGTACCCTCGAGcaccaccaccaccaccac

tga

2.2 RECOMBINANT GENE EXPRESSION AND PROTEIN PURIFICATION

eSrtA(2A-9) and (4S-9) pET29b were gifts from David Liu (2A-9: Addgene plasmid # 75145; http://n2t.net/addgene:75145; RRID:Addgene_75145; 4S-9: Addgene plasmid # 75146; http://n2t.net/addgene:75146; RRID:Addgene_75146).

All relevant plasmids (eSrtA 2A-9, eSrtA 4S-9, pET21 mRuby-LAETG-6xHis, and pET21 mCerulean-LPESG-6xHis) were isolated from 5 mL 37 °C overnight cultures and used to transform BL21 (DE3) cells for protein purification. The transformed BL21 lines were used to inoculate 5 mL starter cultures in LB with the respective selection antibiotic (carbenicillin at 0.1 mg/mL or kanamycin at 0.05 mg/mL), maintained overnight at 37 °C and 200+ RPM. The cultures were scaled up the next day to 400 mL LB (with antibiotic at standard final concentration) and

recombinant gene expression was induced with 0.5 µM isopropyl β-D-1-thiogalactopyranoside (IPTG) at an OD600 of 0.6-0.8 at 16C for 16+ hours. Cells were pelleted at 4000 rpm and resuspended in 40 mL lysis buffer (20 mM Tris, 50 mM NaCl, 10 mM imidazole, pH 7.5) and sonicated in an ice bath (3 minutes sonication, 30% amplitude, 33% duty cycle, and 3 minutes of rest, 6 cycles total). Lysates were centrifuged at 4000 rpm for 20 minutes to pellet insoluble fractions.

Sorting signal-tagged fluorescent proteins (mCerulean-LPESG-6xHis, mRuby-LAETG-6xHis) and eSrtAs (2A-9 and 4S-9) were purified from clarified lysates via nickel affinity chromatography. Lysates were added to lysis buffer-equilibrated nickel-nitrilotriacetic acid (Ni-NTA) agarose resin (3 mL, GoldBio) and histidine-tagged target proteins left to bind at 4 °C for 1 hour on a rocker. Beads were washed five times with 20 mL wash buffer (20 mM Tris, 50 mM NaCl, 20 mM imidazole, pH 7.5). Target proteins were eluted in a 50 mM imidazole elution buffer (20 mM Tris, 50 mM NaCl, pH 7.5) and dialyzed against an imidazole-free buffer (20 mM Tris, 50 mM NaCl, pH 7.5) with SnakeSkin Dialysis tubing (MWCO 10 kDa, Thermo Fisher). Purified protein was concentrated in Amicon centrifugal filter units (MWCO 10 kDa, Millipore).

Purified protein samples were analyzed by SDS-PAGE (in Tris-Glycine running buffer) after 1:1 dilution with 2X Laemmli reducing sample buffer, heating at 95 °C for 10 minutes, and centrifugation at 10,000 rpm for 10 minutes.

2.3 SYNTHESIS OF PREVIOUSLY REPORTED COMPOUNDS USED IN THIS WORK

Many components of the PEG-based hydrogels were synthesized as previously reported (Figure 2.1).

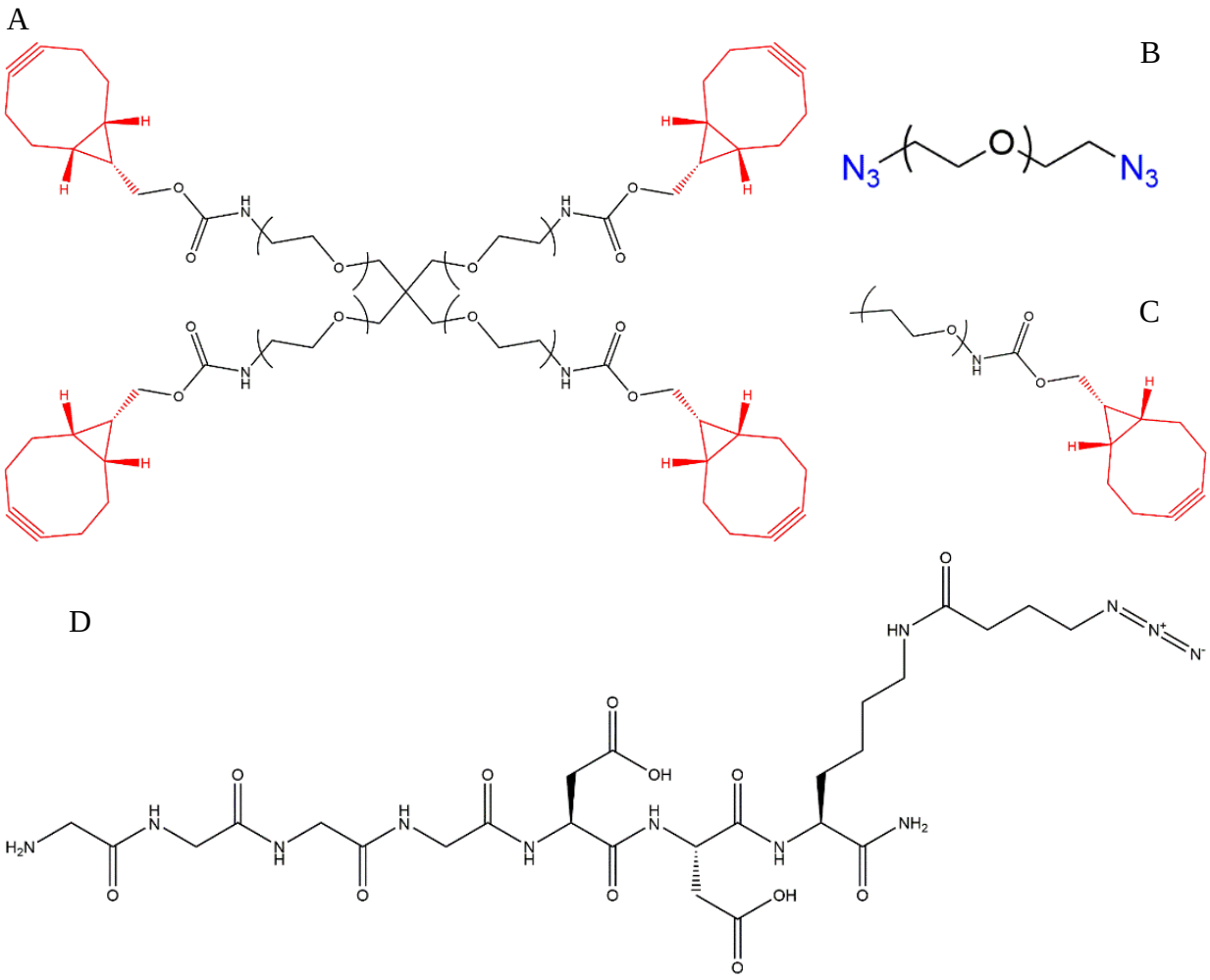

Figure 2.1. A) Poly(ethylene glycol) tetrabicyclononyne (PEG-tetraBCN, M_n ~ 20,000 Da), B) poly(ethylene glycol) diazide (N_3-PEG-N_3, M_n ~ 3,400 Da), C) methoxy poly(ethylene glycol) bicycloononyne (mPEG-BCN, Mn ~ 2,000 Da or 5,000 Da), and D) H-GGGGDDK(N_3)-NH_2 peptide were synthesized as previously reported.[15,30]

2.4 EVOLVED SORTASE-MEDIATED AZIDE FUNCTIONALIZATION OF SORTING SIGNAL-CONTAINING FLUORESCENT PROTEINS

2.4.1 *Synthesis of mCerulean-LPESG-GGGDDK(N3)*

H-GGGGDDK(N_3)-NH_2 (10 mM) was reacted with mCerulean-LPESG-6xHis (100 µM) and eSrtA 4S-9 (20 µM), with glycerol and calcium chloride supplemented to a final concentration of 10 mM each, in a total reaction volume of 300 µL, for one hour at 37 °C , pH ~7.5, and 200 rpm on a shaker-incubator. Ni-NTA agarose beads were used to filter out unreacted mCerulean-LPESG-6xHis, after equilibration (3x, 500x*g*, 1 min. wash) in lysis buffer (10 mM imidazole, 20 mM Tris, 50 mM NaCl.) 120 µL of Ni-NTA agarose slurry was added to the 300 µL reaction volume and left to bind unreacted mCerulean-LPESG-6xHis at 4 °C for 1 hour, on a rocker. The slurry was then passed through Pierce spin columns (Thermo Fisher) to filter out beads. The binding and filtration steps were repeated once before the reaction products were passed through Zeba spin desalting columns (7k MWCO, Thermo Fisher), following manufacturer protocols for buffer exchange, for further purification of mCerulean-LPESG-GGGDDK(N_3)-NH_2 (e.g., to exclude any remaining unreacted H-GGGGDDK(N_3)-NH_2).

2.4.2 *Synthesis of mRuby-LAETG-GGGDDK(N3)*

H-GGGGDDK(N_3)-NH_2 (10 mM) was reacted with mRuby-LAETG-6xHis (100 µM) and eSrtA 2A-9 (20 µM), with glycerol and calcium chloride supplemented to a final concentration of 10 mM each, in a total reaction volume of 300 µL, for two hours at 37 °C, pH ~7.5, and 200 rpm on a shaker-incubator. Ni-NTA agarose beads were used to filter out unreacted mRuby-LAETG-6xHis, after equilibration (3x, 500x*g*, 1 min. wash) in lysis buffer (10 mM imidazole, 20 mM Tris, 50 mM NaCl.) 120 µL of Ni-NTA agarose slurry was added to the 300 µL reaction volume and

left to bind unreacted mRuby-LAETG-6xHis at 4 °C for 1 hour, on a rocker. The slurry was then passed through Pierce spin columns (Thermo Fisher) to filter out beads. The binding and filtration steps were repeated once before the reaction products were passed through Zeba spin desalting columns (7k MWCO, Thermo Fisher), following manufacturer protocols for buffer exchange, for further purification of mRuby-LAETG-GGGDDK(N_3)-NH_2.

2.4.3 *Gel shift assays to confirm SPAAC reactivity of azide-functionalized proteins*

Azide-functionalized fluorescent proteins (mCerulean-LPESG-GGGDDK(N_3)-NH_2 and mRuby-LAETG-GGGDDK(N_3)-NH_2) were reacted with mPEG-BCN in a 1:100 molar ratio, in 12 µL reactions (STEPL buffer) at 4 °C on a rocker, overnight. Reactions were then combined in a 1:1 volume ratio with 2X Laemmli reducing sample buffer and heated at 95 °C for 10 minutes before analysis by SDS-PAGE.

2.5 SYNTHESIS OF GELS FOR PROTEIN RELEASE

2.5.1 *Precursor reactions for protein-functionalized PEG-based hydrogels*

Gel precursor solutions were left to react at 4 °C overnight on a rocker, containing 5 mM PEG-tetraBCN (20k) and 7.5 µM azide-functionalized fluorescent protein(s) in STEPL buffer (20 mM Tris, 50 mM NaCl). For gels containing both mRuby-LAETG-GGGDDK(N_3)-NH_2 and mCerulean-LPESG-GGGDDK(N_3)-NH_2, final concentrations of both proteins in the precursor reaction solution was 7.5 µM.

2.5.2 *SPAAC crosslinking and washing of PEG-based hydrogels*

Precursor solutions were mixed and centrifugally pulsed with stoichiometrically matched quantities of PEG-diazide (3.4k) crosslinker to the expected ratio of unreacted BCN groups of

PEG-tetraBCN (20k), so that the final concentration of PEG-tetraBCN in the gel would be 4 mM and that of proteins 6 µM. 10 µL of the pre-gel solution was pipetted into the bottom of tissue culture-treated 96-well plates (Genesee Scientific). Gels were left to crosslink at room temperature for one hour. Gels were then washed three times in STEPL buffer at 4 °C, 200 µL/well, for 72+ hours each. All wash solutions were collected and stored at -20 °C before analysis.

2.6 ENZYMATICALLY TRIGGERED PROTEIN RELEASE AND CHARACTERIZATION

2.6.1 *Reaction conditions for comparisons of eSrtA-triggered protein release from hydrogels*

150 µL reaction solutions were prepared in master mixes for all test conditions except sequential release (2A-9 added before 4S-9 and vice versa), containing 60 µM eSrtA 2A-9, 4S-9, or both (each 60 µM); 2.5 mM Ca^{2+}; 600 µM triglycine; 20% w/v glycerol; and brought up to volume by STEPL buffer. For sequential release, component volumes for reaction solutions were similarly calculated for a final volume of 150 µL, but master mixes prepared without the second sortase to be added and aliquoted to account for the missing volume. After removal of the last wash, reaction solutions were added to respective 10 µL gels (with each test condition in triplicate). The microplate was wrapped in parafilm and left at 37 °C on a shaker at ~40 rpm.

2.6.2 *Quantifying protein release by fluorescence signal*

At each timepoint, 50 µL each of the reaction solutions was transferred to a black-bottom microplate, analyzed with the BioTek Cytation 5 fluorescent plate reader with settings for mCerulean ($\lambda_{excitation} = 433$, $\lambda_{emission} = 475$) and mRuby ($\lambda_{excitation} = 558$, $\lambda_{emission} = 640$), and returned to the plated gels. Signals were converted to estimated concentrations with functions estimated from standard curves (Figure 2.2.)

A.

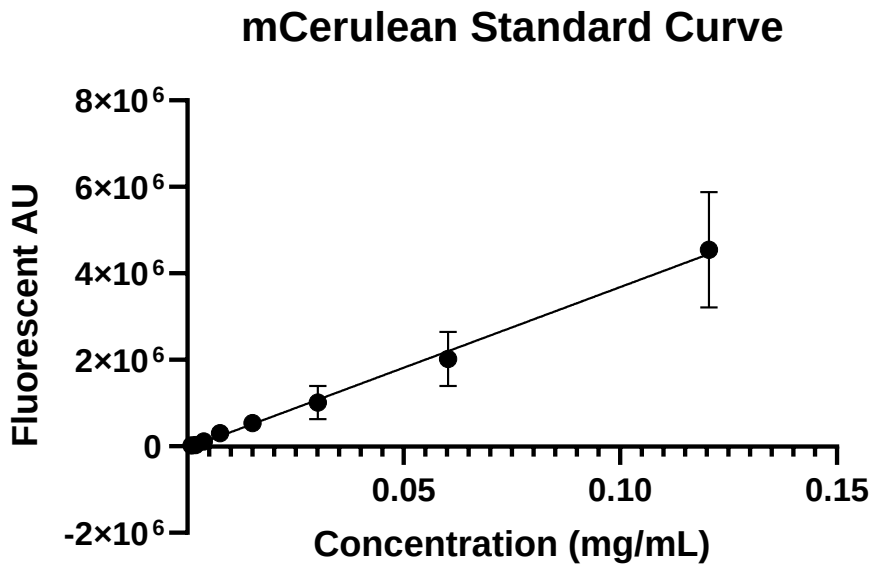

B.

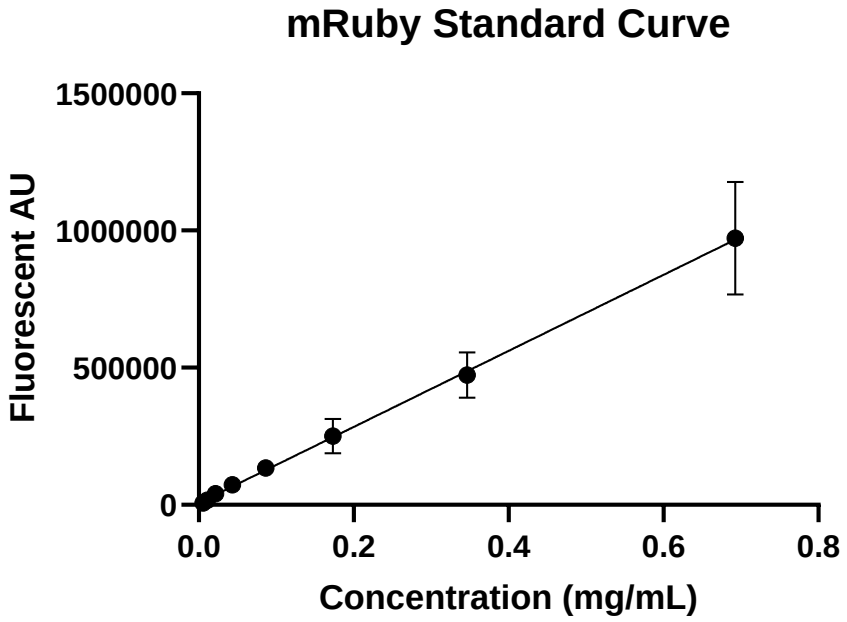

Figure 2.2. Standard curves were prepared from serial dilutions of A) mCerulean-LPESG-6xHis and B) mRuby-LAETG-6xHis (in STEPL buffer, n=3).

Chapter 3. RESULTS AND DISCUSSION

We tested the application of evolved sortases 2A-9 and 4S-9 in modulating biochemical cues presented in hydrogels independent of mechanical properties. With the ultimate goal of triggering release of full-length proteins from PEG-based hydrogels, eSrtAs 2A-9 and 4S-9 were used twice throughout this work; we first exploited these enzymes for the site-specific introduction azide handles onto full-length proteins for SPAAC-driven immobilization in PEG-based hydrogels.

3.1.1 *Construction of sorting signal-containing fluorescent proteins, protein purification for resulting constructs and evolved sortases*

In order to manipulate full-length proteins with eSrtAs 2A-9 and 4S-9, site-directed mutagenesis was applied to two distinct fluorescent proteins (mRuby and mCerulean), for the incorporation of orthogonal sortase substrates, LAETG (eSrtA 2A-9) and LPESG (eSrtA 4S-9), and hexahistidine tags for nickel affinity purification (Figure 3.1).

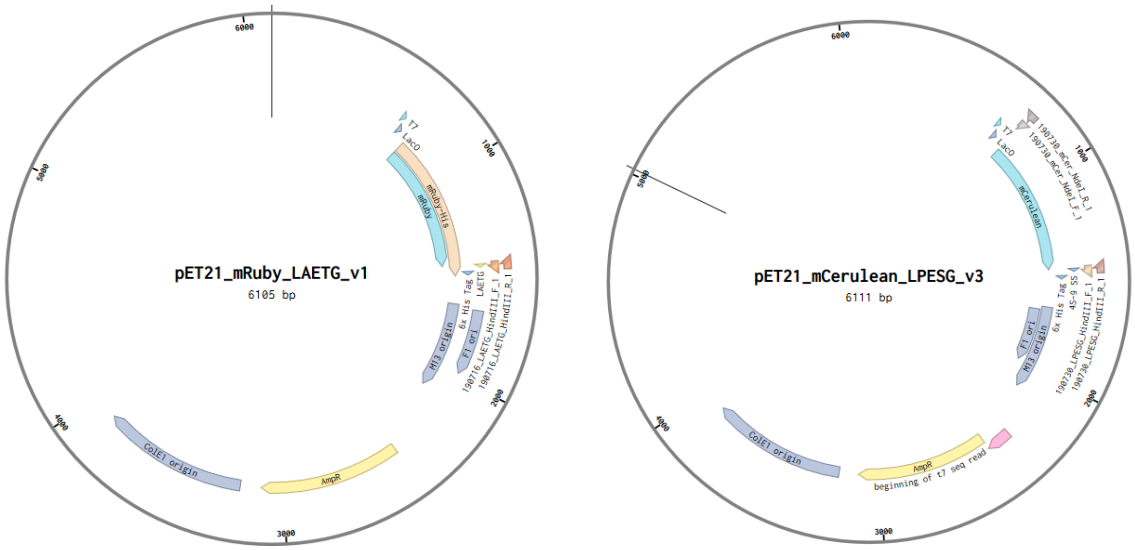

Figure 3.1. Plasmid maps of final fluorescent proteins containing relevant sorting signals and hexahistidine tags.

After confirming the sequences of the cloned constructs, eSrtA 2A-9, eSrtA 4S-9, mCerulean-LPESG-6xHis, and mRuby-LAETG-6xHis were expressed in *E. coli* and successfully purified by nickel affinity chromatography, with purity and non-aggregation demonstrated through SDS-PAGE analysis of soluble fractions (Figure 3.2.)

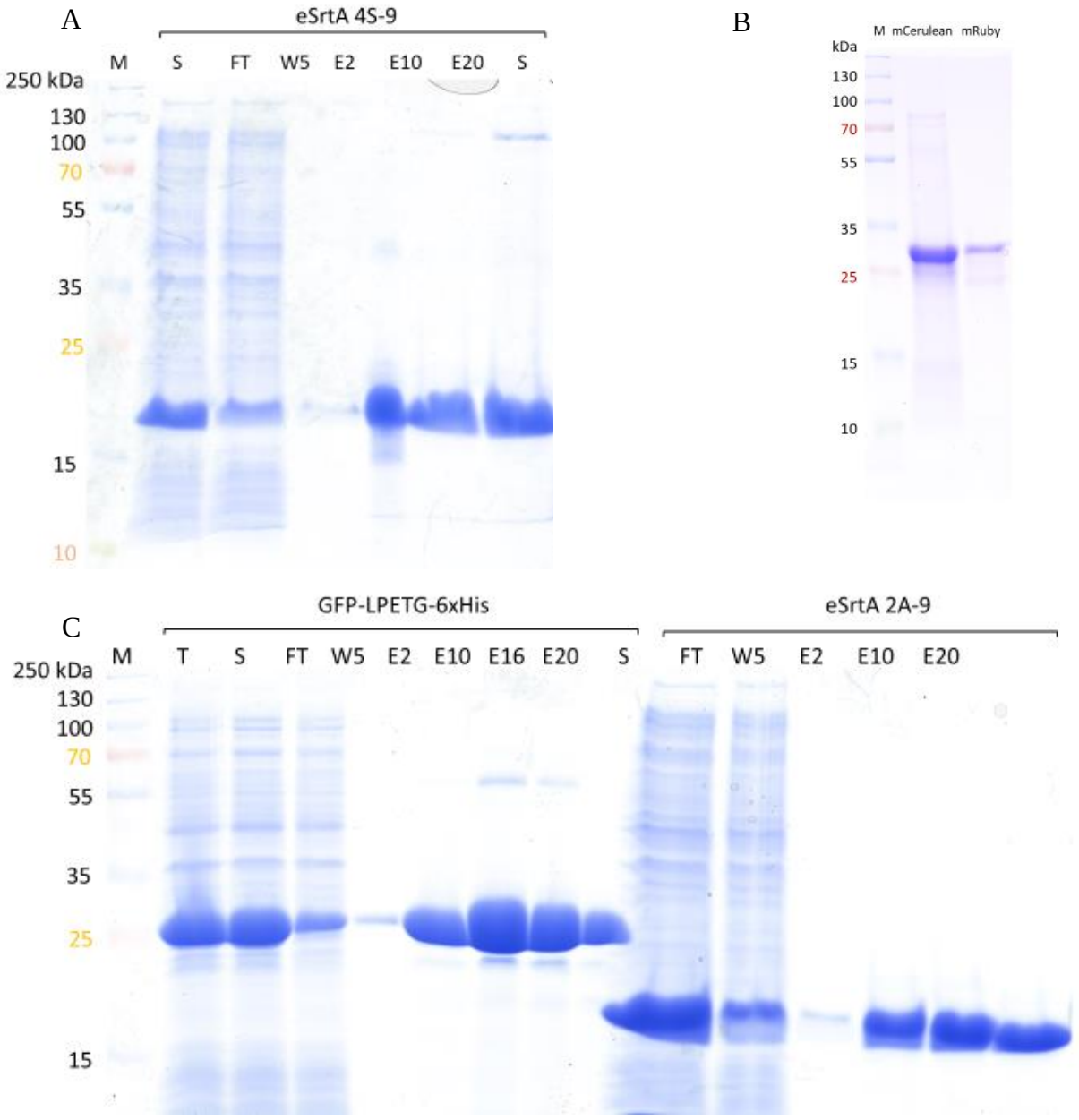

Figure 3.2. SDS-PAGE results for A) eSrtA 4S-9; B) mCerulean-LPESG-6xHis and mRuby-LAETG-6xHis; C) GFP-LPETG-6xHis (not used in this thesis) and eSrtA 2A-9. Expected masses of eSrtAs 2A-9 and 4S-9 was 18 kDa; for fluorescent proteins mCerulean-LPESG-6xHis and mRuby-LAETG-6xHis, expected masses were 29 kDa.

We also confirmed that molecular weights of purified proteins and a short peptide needed to introduce azide-functionality and serve as a secondary eSrtA substrate, H-GGGGDDK(N_3)-NH_2 (prepared through solid-phase synthesis), are as expected. The molecular weights of eSrtA 2A-9, eSrtA 4S-9, mCerulean-LPESG-6xHis, mRuby-LAETG-6xHis, and H-GGGGDDK(N_3)-NH_2 were confirmed by liquid chromatography-mass spectrometry (LC-MS, Figure 3.3).

A.

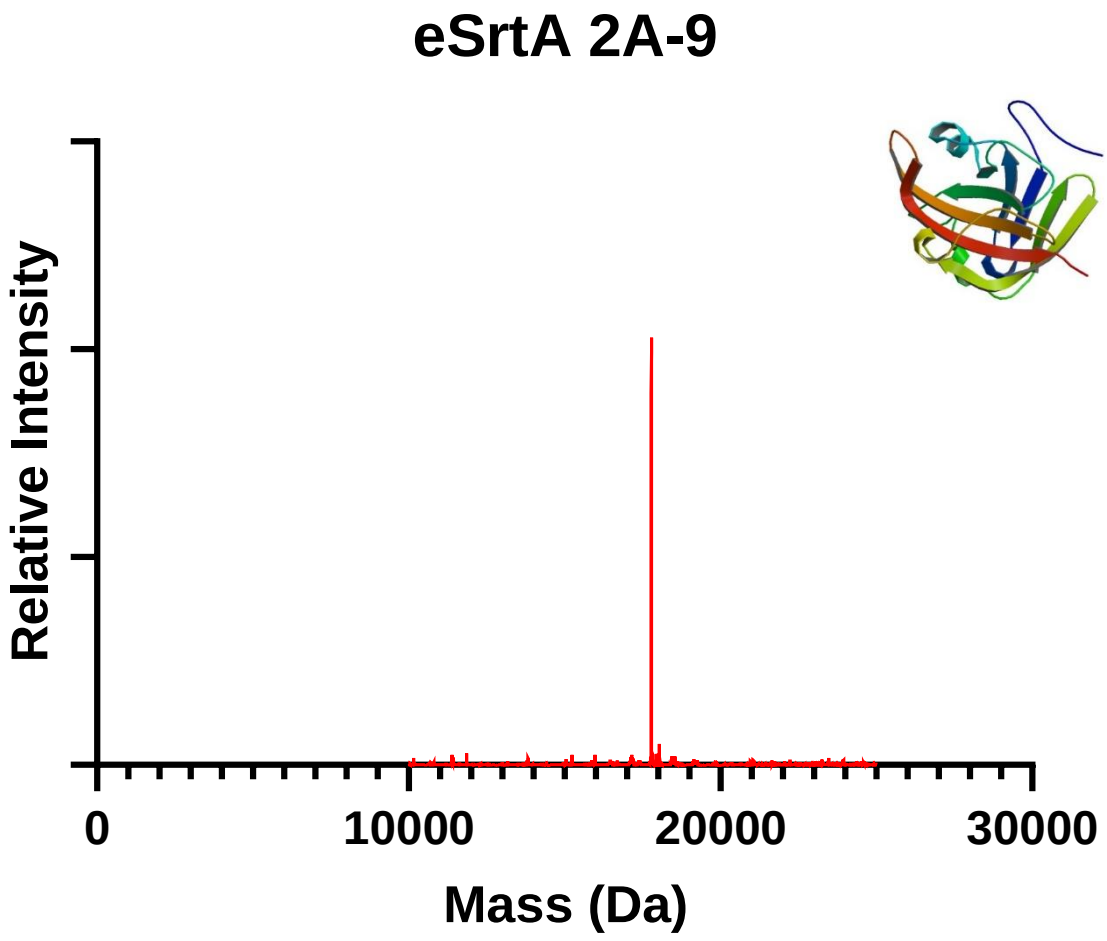

B.

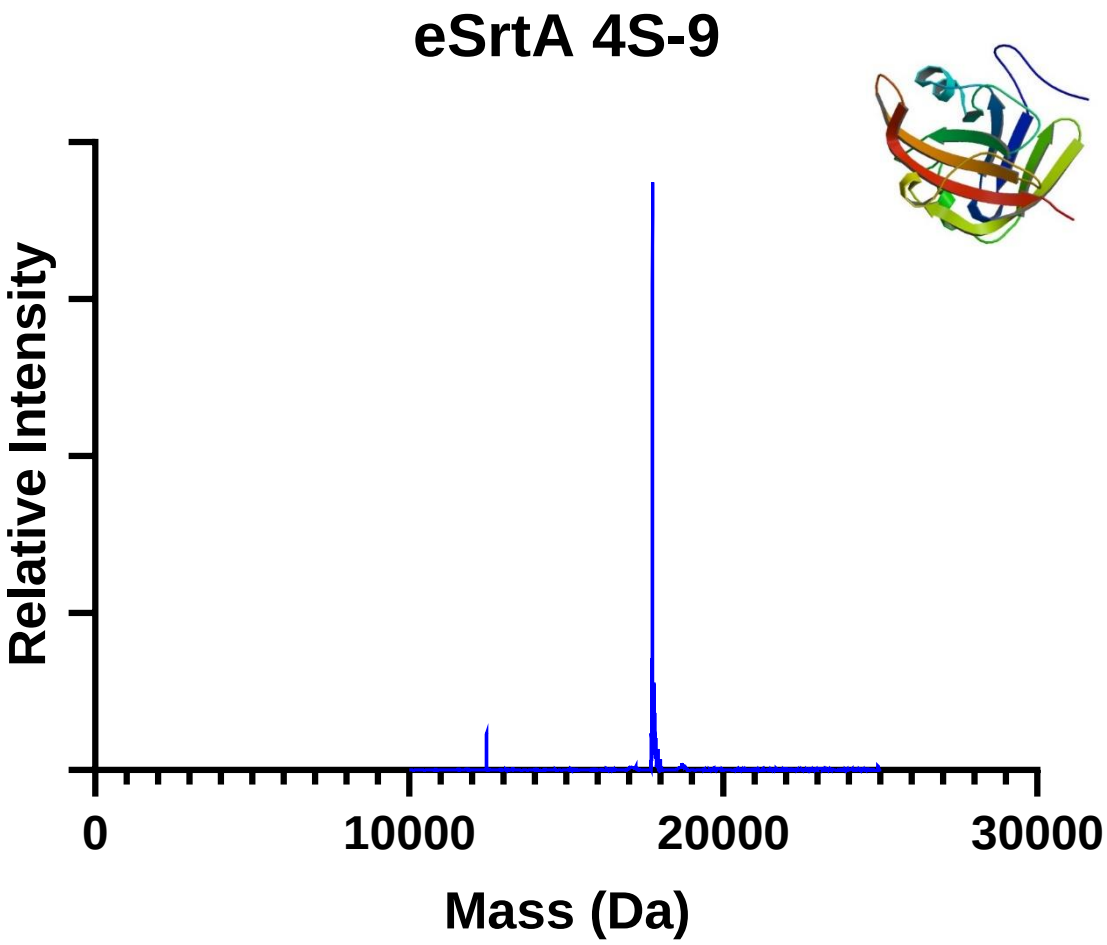

C.

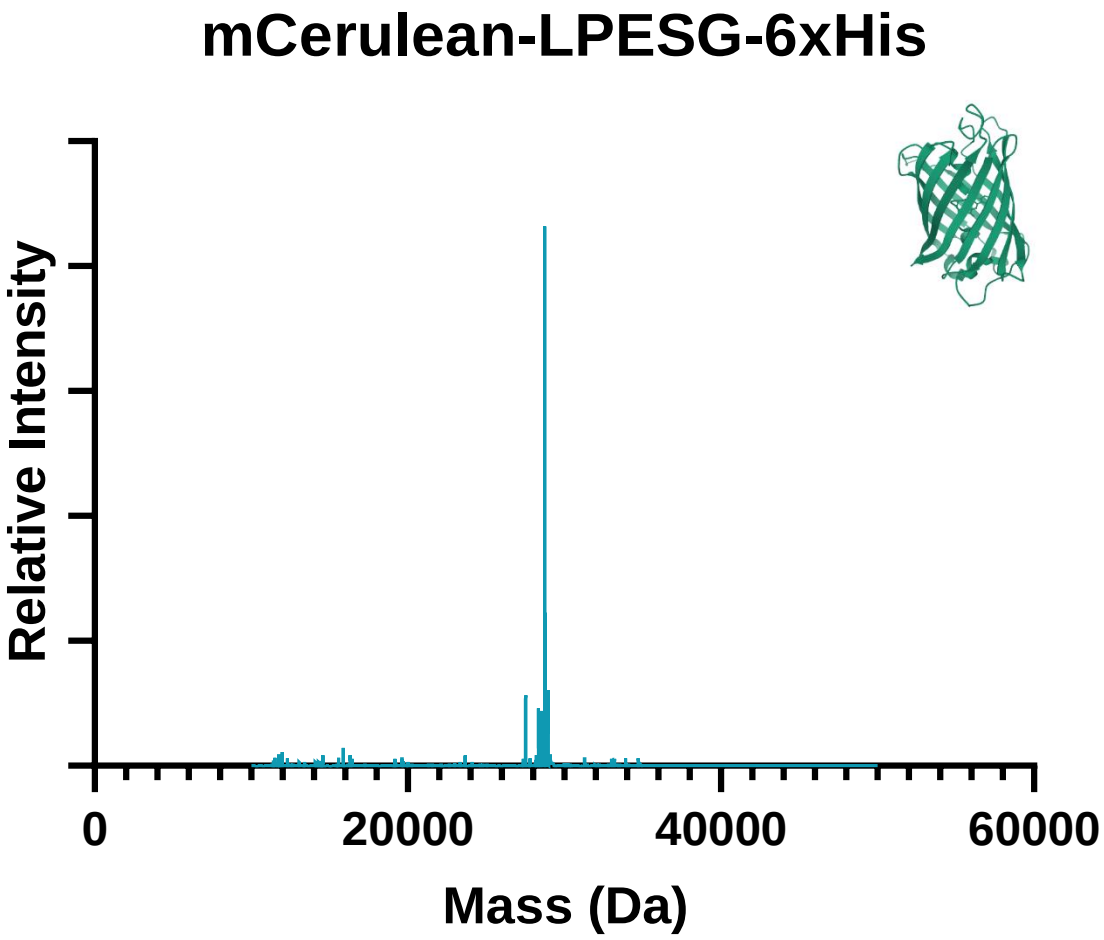
mCerulean-LPESG-6xHis
Relative Intensity
0
20000
40000
60000
Mass (Da)

D.

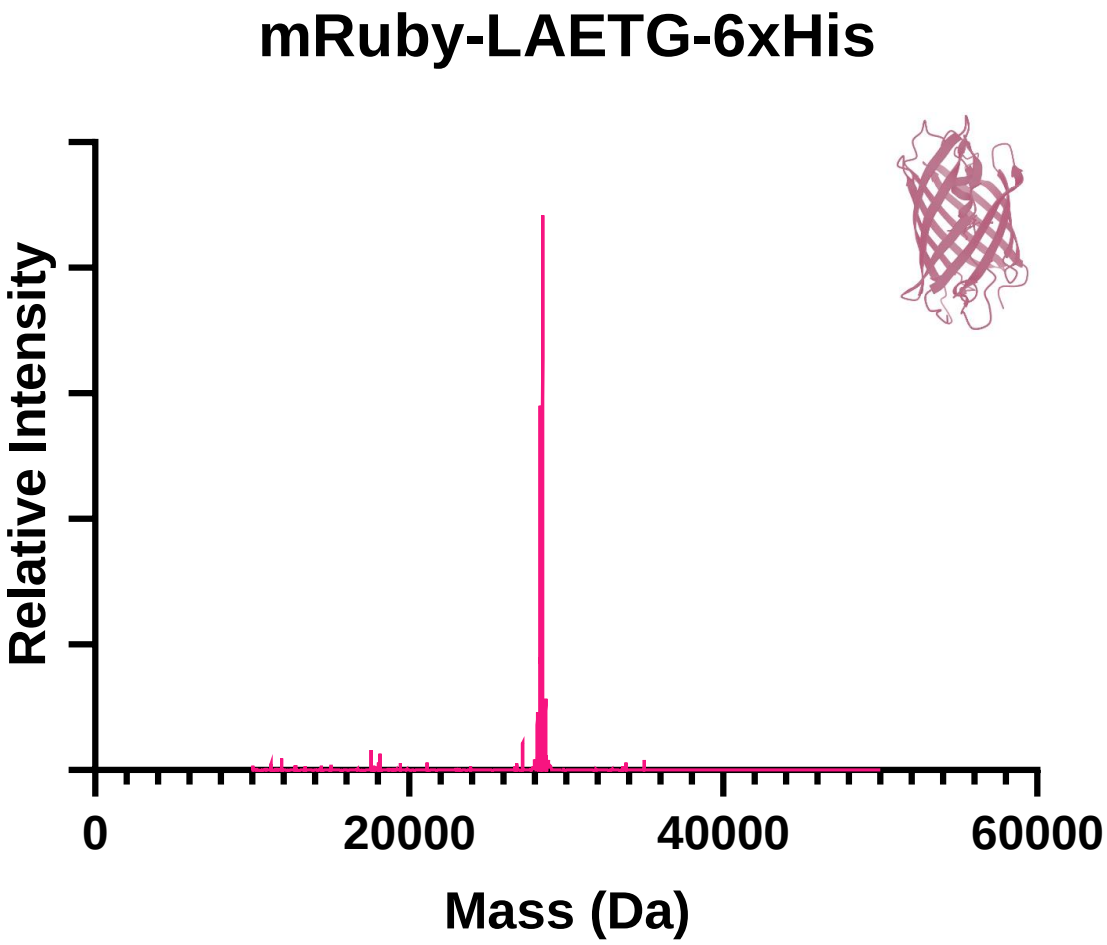
mRuby-LAETG-6xHis
Relative Intensity
0
20000
40000
60000
Mass (Da)

E.

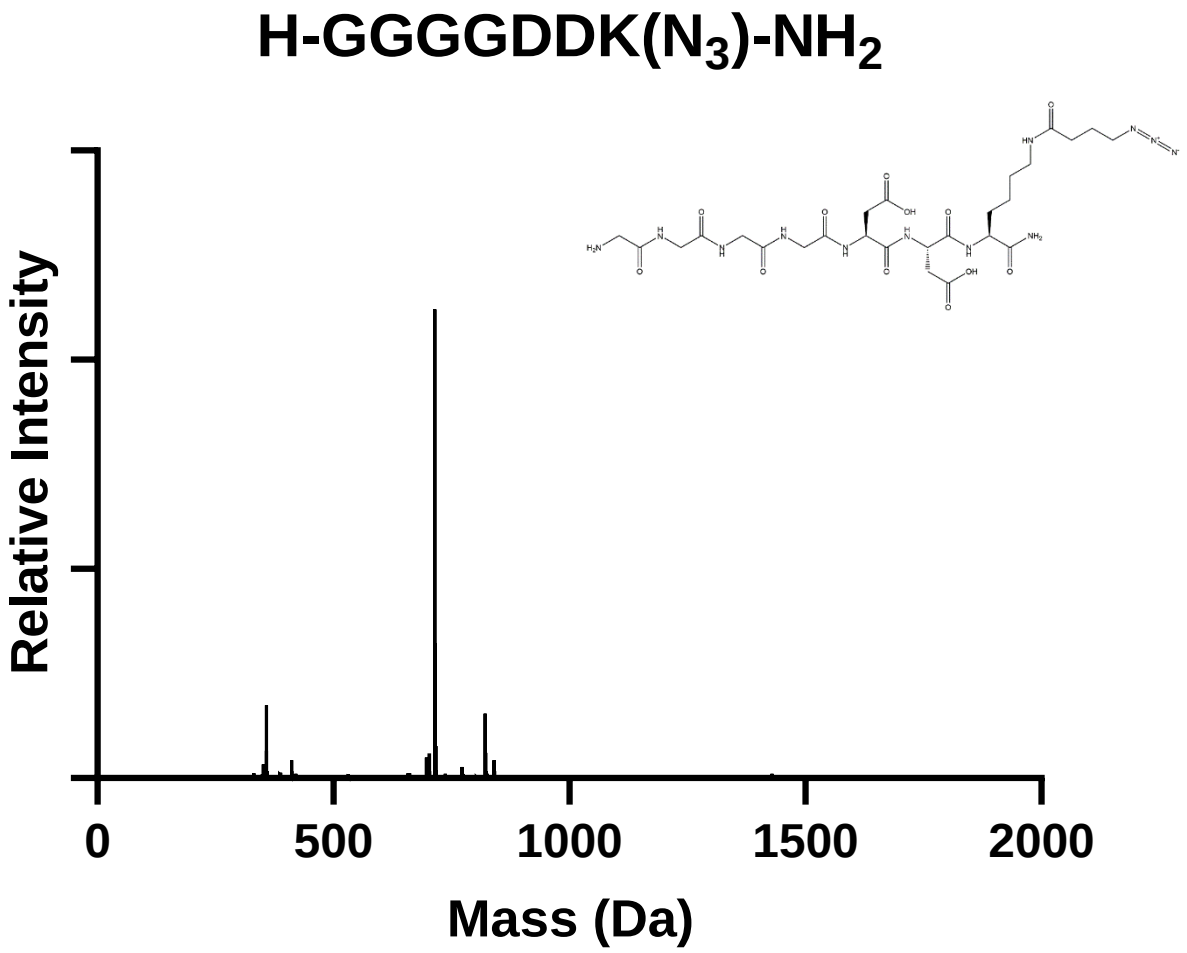

Figure 3.3. LC-MS confirmation of molecular weights for all purified proteins and H-GGGGDDK(N_3)-NH_2. A) eSrtA 2A-9 spectrum, with a dominant peak (17.787 kDa) matching expected mass for translated sequence (17.79 kDa). B) eSrtA 4S-9 spectrum, with a dominant peak (17.751 kDa) matching expected mass for translated sequence (17.75 kDa). C) mCerulean-LPESG-6xHis spectrum, with a dominant peak (28.753 kDa) near matching expected mass calculation for sum of mCerulean and peptide tag masses (28.762 kDa). D) mRuby-LAETG-6xHis spectrum, with a dominant peak (28.504 kDa) near matching expected mass calculation for sum

of mRuby and peptide tag masses (28.512 kDa). E) H-GGGGDDK(N_3)-NH_2 spectrum, with a dominant peak matching expected mass calculation +1H (715.3 Da).

3.1.2 *Sortase-catalyzed azide functionalization of full-length proteins*

In order to site-specifically introduce an azide group onto the previously constructed sorting signal-containing fluorescent proteins, eSrtAs 2A-9 and 4S-9 were used to react the second substrate H-GGGGDDK(N_3)-NH_2 with acyl group donors mCerulean-LPESG-6xHis and mRuby-LAETG-6xHis in aqueous reaction conditions. Purification of the targeted products (mCerulean-LPESG-GGGDDK(N_3)-NH_2 and mRuby-LAETG-GGGDDK(N_3)-NH_2, also referred to as mCerulean-LPESG-N_3 and mRuby-LAETG-N_3 respectively) was enabled by nickel affinity purification of unreacted fluorescent proteins (with hexahistidine tags), size exclusion of unreacted or byproduct short peptides, and buffer exchange to remove other unwanted small molecules or ions (Figure 3.4.)

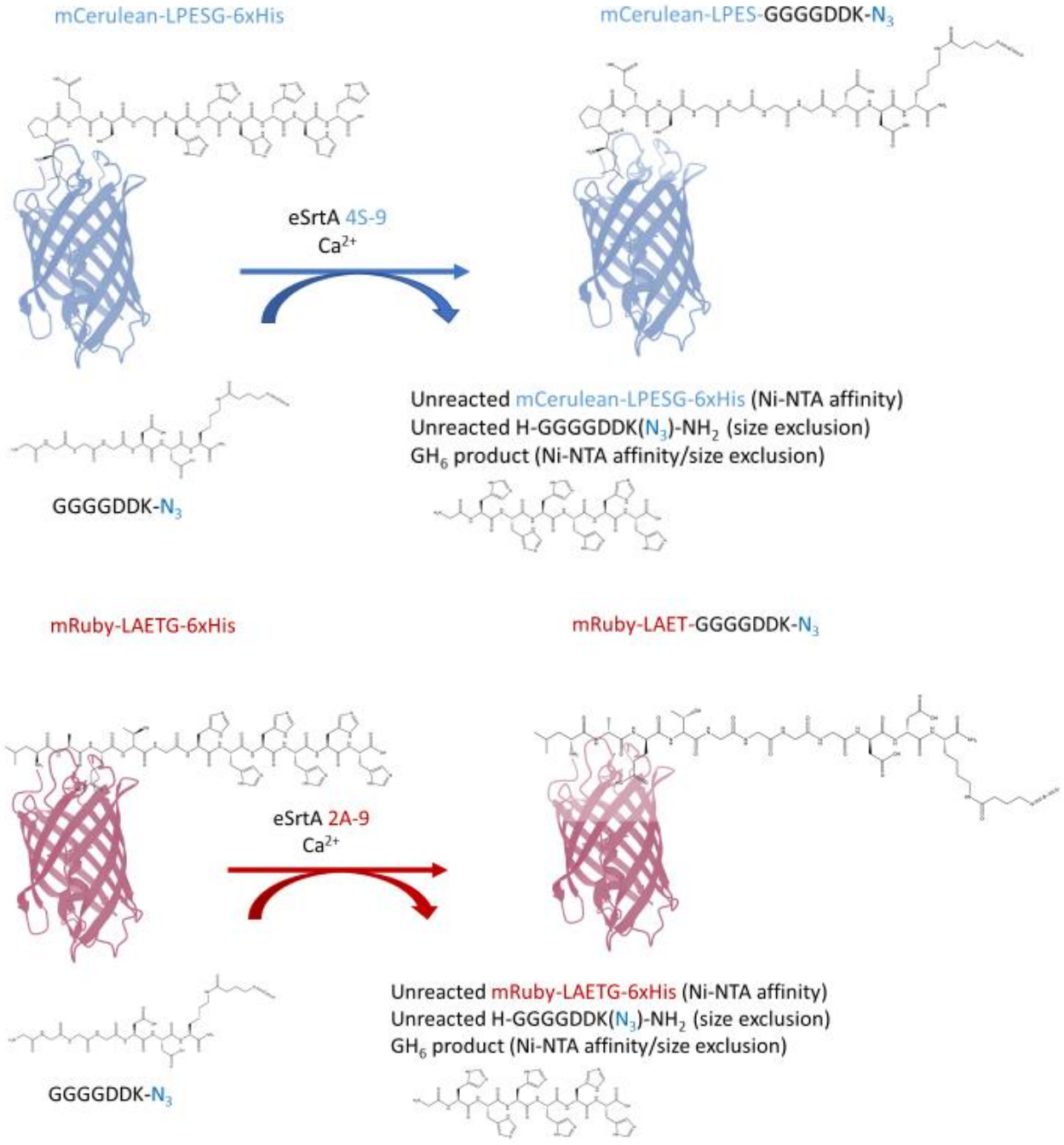

Figure 3.4. Reactions for sortagging fluorescent proteins with azide groups.

Presence of intended products mCerulean-LPESG-N_3 and mRuby-LAETG -N_3 was confirmed by LC-MS (Figure 3.5).

A.

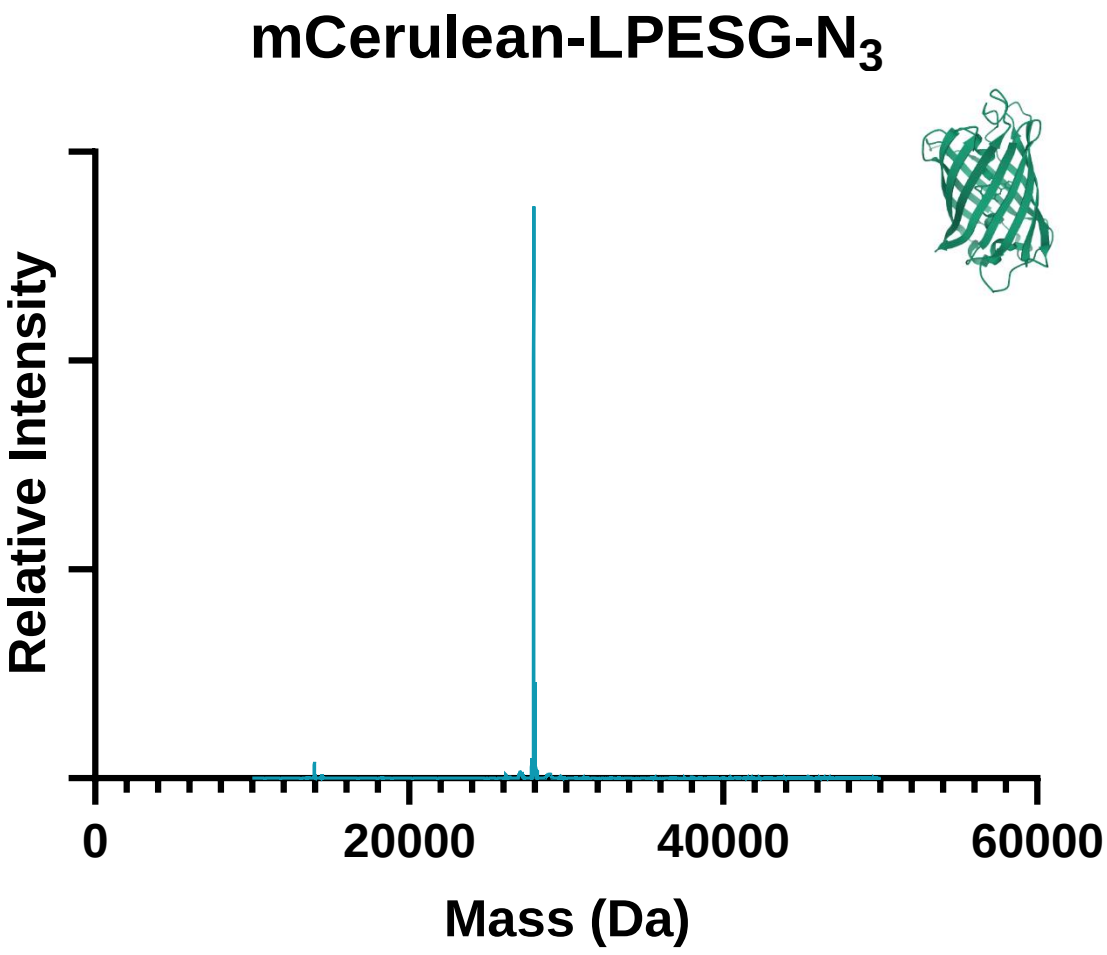
mCerulean-LPESG-N3
Relative Intensity
0
20000
40000
60000
Mass (Da)

B.

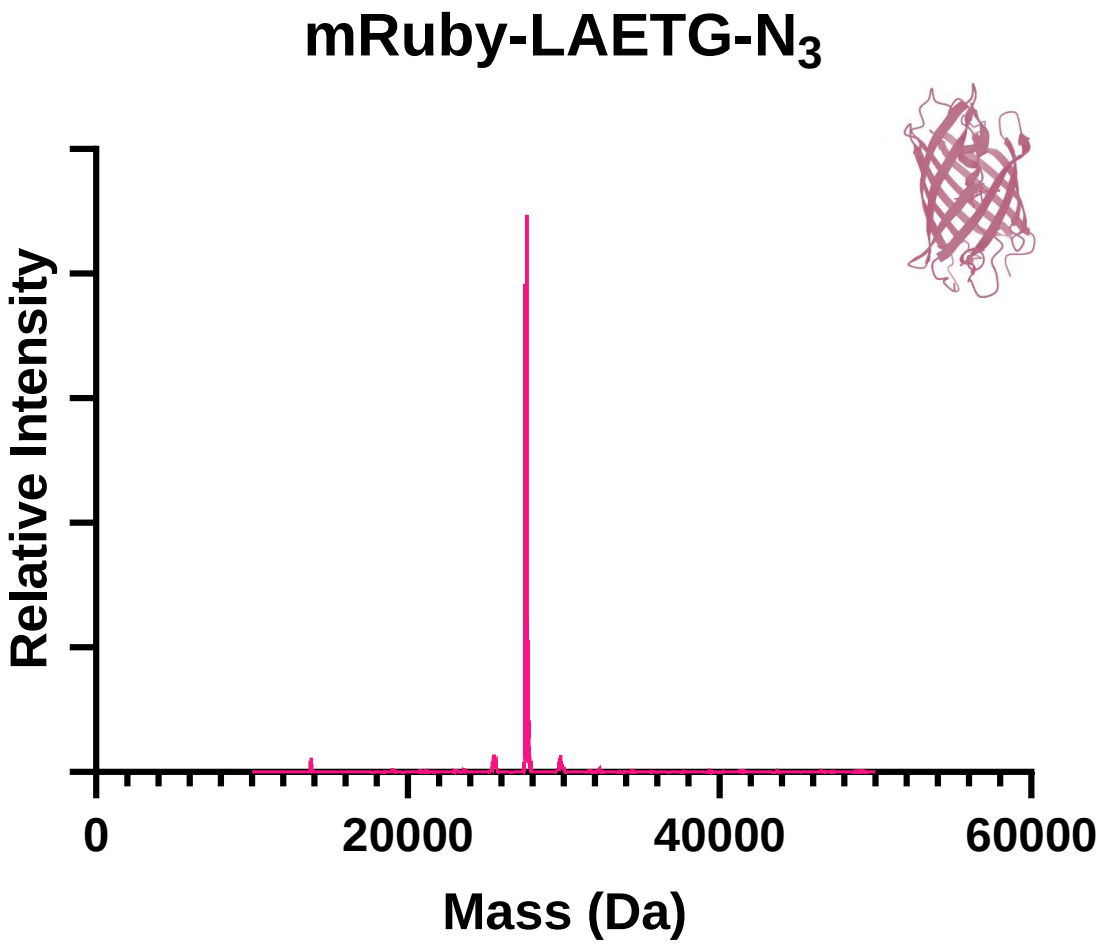

Figure 3.5. A) LC-MS confirmation of mCerulean-LPESG-GGGDDK-N3 mass (expected 27.910 kDa, observed 27.936 kDa for dominant peak). B) LC-MS confirmation of mRuby-LAETG-GGGDDK-N3 mass (expected 27.626 kDa, observed 27.650 for dominant peak).

SPAAC reactivity of azide-functional fluorescent proteins was confirmed with a mPEG(10k)-BCN gel shift assay, in which proteins were PEGylated and observed to upshift in mass by ~10 kDa as expected (Figure 3.6.)

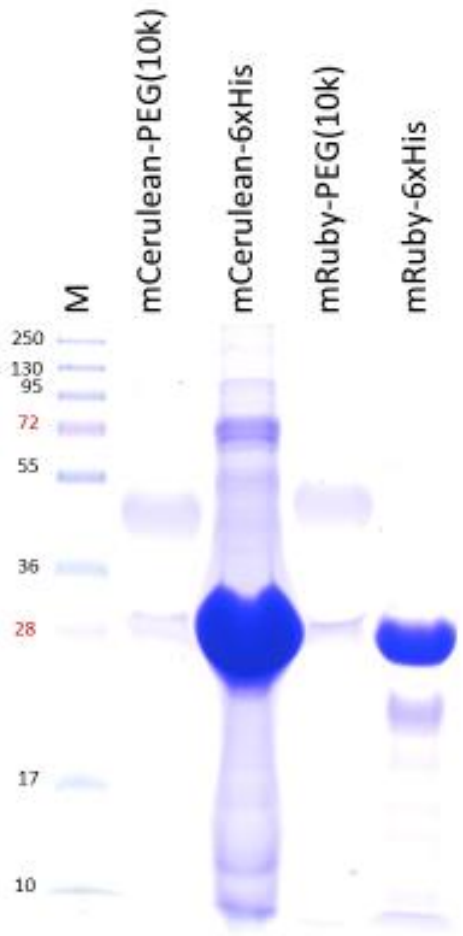

Figure 3.6. SDS-PAGE gel shift assay to confirm SPAAC reactivity of mCerulean-LPESG-GGGDDKN3 and mRuby-LAETG-GGGDDKN3 with mPEG-BCN.

3.1.3 *Selective protein release by orthogonal eSrtAs from PEG-based hydrogels*

Having confirmed successful generation and SPAAC reactivity of mRuby-LAETG-N_3 and mCerulean-LPESG-N_3, the azide-functionalized fluorescent proteins were reacted via SPAAC with a gel precursor, PEG-tetraBCN, before crosslinking of gels with PEG-diazide to covalently tether the proteins within PEG-based hydrogels (Figure 3.7). Gels were washed for several days three times to remove unincorporated fluorescent protein. Selectivity and kinetics were then tested

of orthogonal eSrtA-catalyzed release of mRuby-LAETG and/or mCerulean-LPESG from the hydrogels.

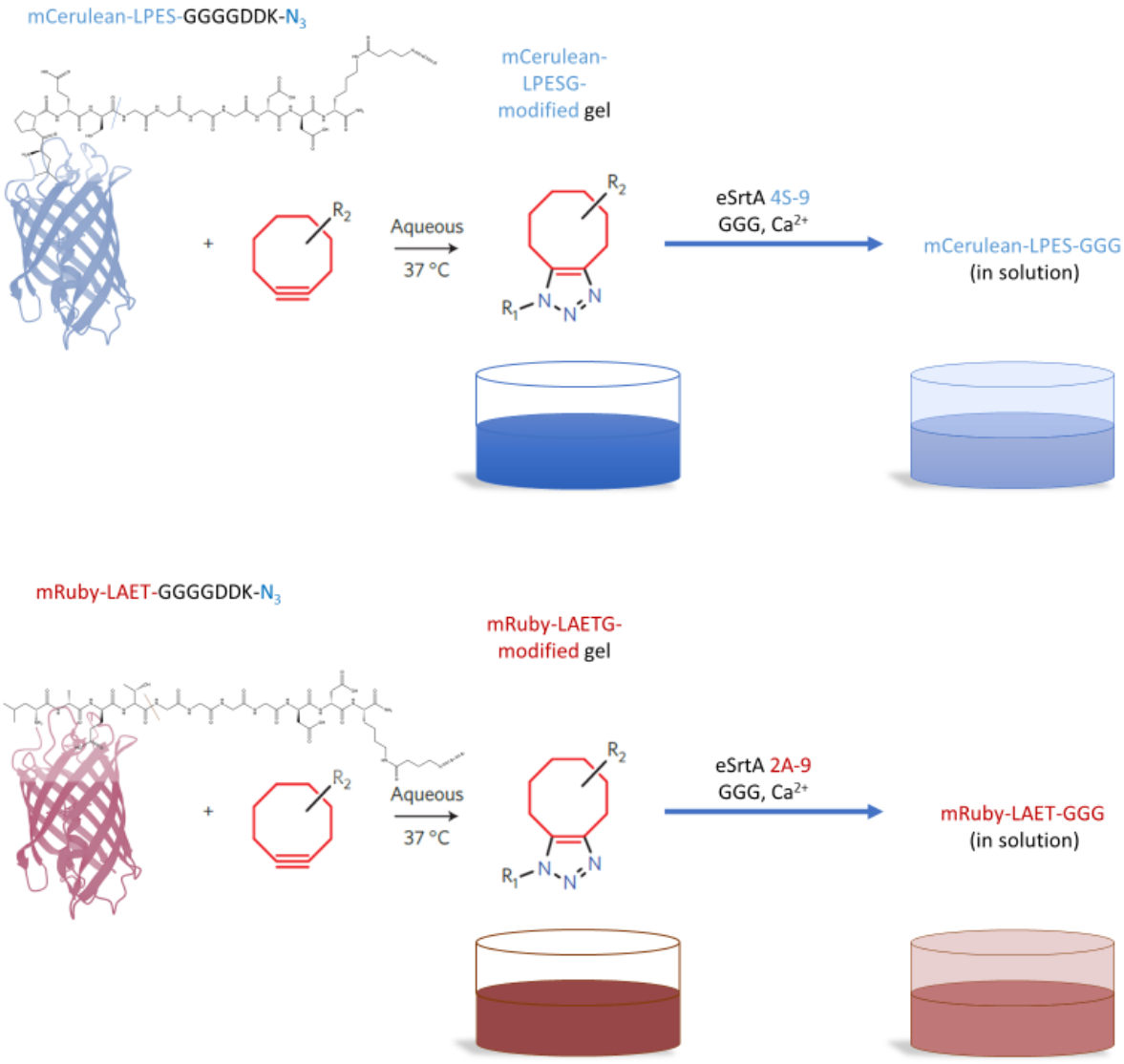

Figure 3.7. Design of eSrtA-triggered protein release experiments: azide-functionalized proteins were covalently immobilized within PEG-based gels using SPAAC, then released by orthogonal eSrtAs in conjunction with calcium and polyglycine.

Activity of both orthogonal sortases for release of mCerulean-LPESG was tested, demonstrating higher effective selectivity of release when only mCerulean-LPESG is tethered within a hydrogel within the time range investigated, of 8 hours, as opposed to when both mCerulean-LPESG and mRuby-LAETG are tethered. In a gel functionalized by only the mCerulean-LPESG protein, eSrtA 4S-9 releases the respective LPESG-containing tethered protein at a faster rate than eSrtA 2A-9 (Figure 3.8). There is negligible release by 2A-9 alone and insignificantly different release when 2A-9 and 4S-9 are both added, as compared to 4S-9 alone (Figure 3.8). However, in a gel containing both mCerulean-LPESG and mRuby-LAETG, release profiles for 2A-9 and 4S-9 are comparable (Figure 3.9). Increasing the protein concentration from 6 μM to 12 μM demonstrates a roughly proportionate increase in protein release, although this was not observed between 3 and 6 μM (Figure 3.10.)

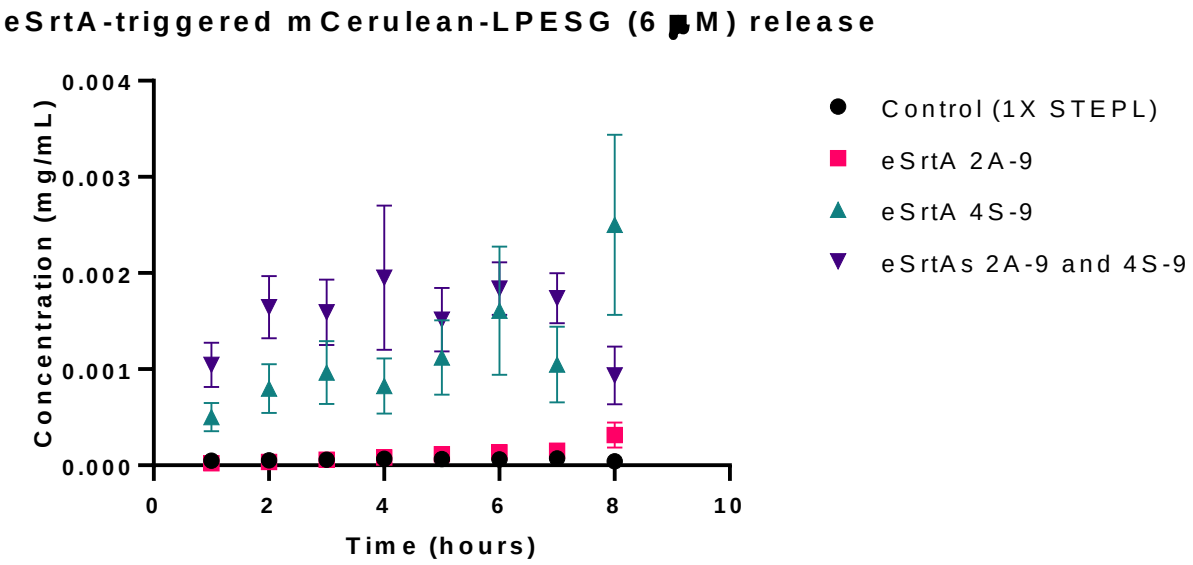

Figure 3.8. Quantification of mCerulean-LPESG released into solution over eight hours, with 10 µL mCerulean-LPESG-tethered gels, initial mCerulean-LPESG concentration of 6 µM, treated with either STEPL buffer (control), eSrtA 2A9, eSrtA 4S9, or both eSrtAs 2A9 and 4S9, in triplicate (error bars denote one standard error of the mean.)

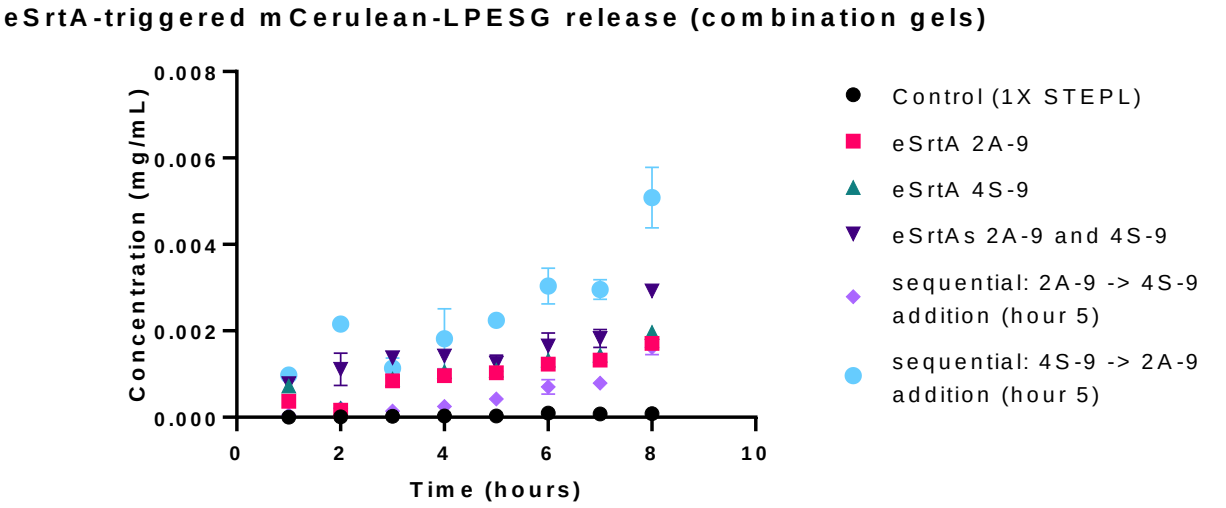

Figure 3.9. Quantification of mCerulean-LPESG released into solution over eight hours, with 10 µL mCerulean-LPESG- and mRuby-LAETG-tethered gels, initial tethered protein concentrations of 6 µM, treated with either STEPL buffer (control), eSrtA 2A9, eSrtA 4S9, both eSrtAs 2A9 and 4S9, or with the two eSrtAs in series (2A-9 for 5 hours before 4S-9 addition and vice versa), in triplicate (error bars denote one standard error of the mean.)

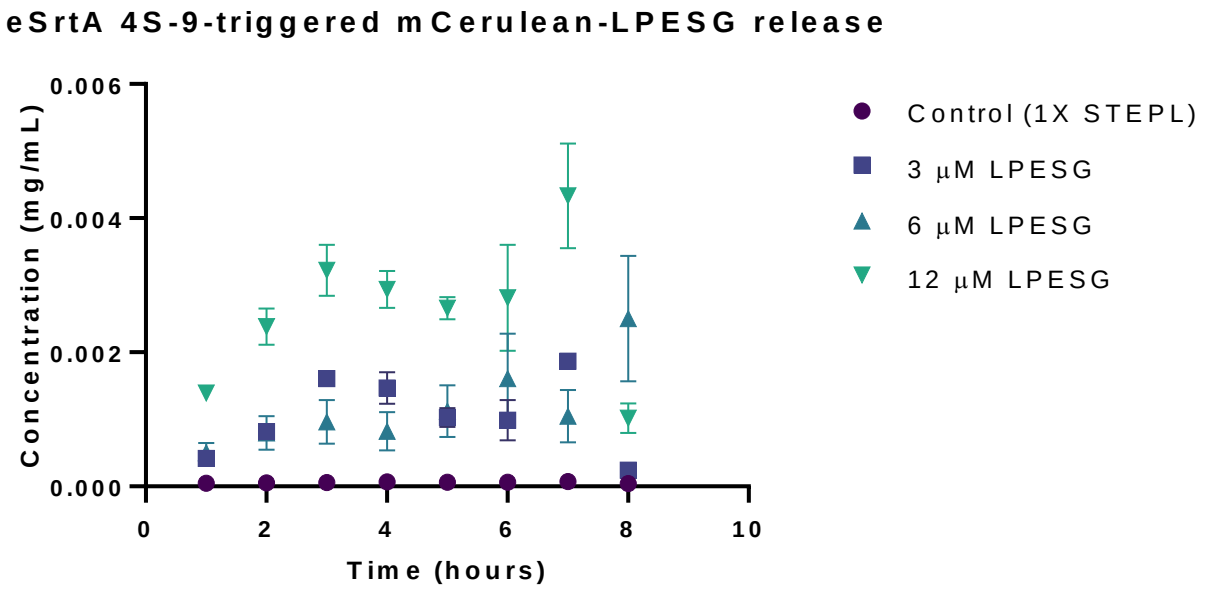

Figure 3.10. Quantification of mCerulean-LPESG released into solution over eight hours, with 10 µL mCerulean-LPESG-tethered gels, initial tethered protein concentrations of 3, 6, or 9 µM, treated with eSrtA 4S-9, in triplicate (error bars denote one standard error of the mean.)

Similar patterns were observed for mRuby-LAETG tethered within hydrogels and tested against both eSrtAs. Greatest orthogonality and control over release was observed in gels with only mRuby-LAETG tethered – eSrtA 2A-9 releases the respective LAETG-containing tethered protein

at a much faster rate than 4S-9 and with a similar profile as both 2A-9 and 4S-9 added together (

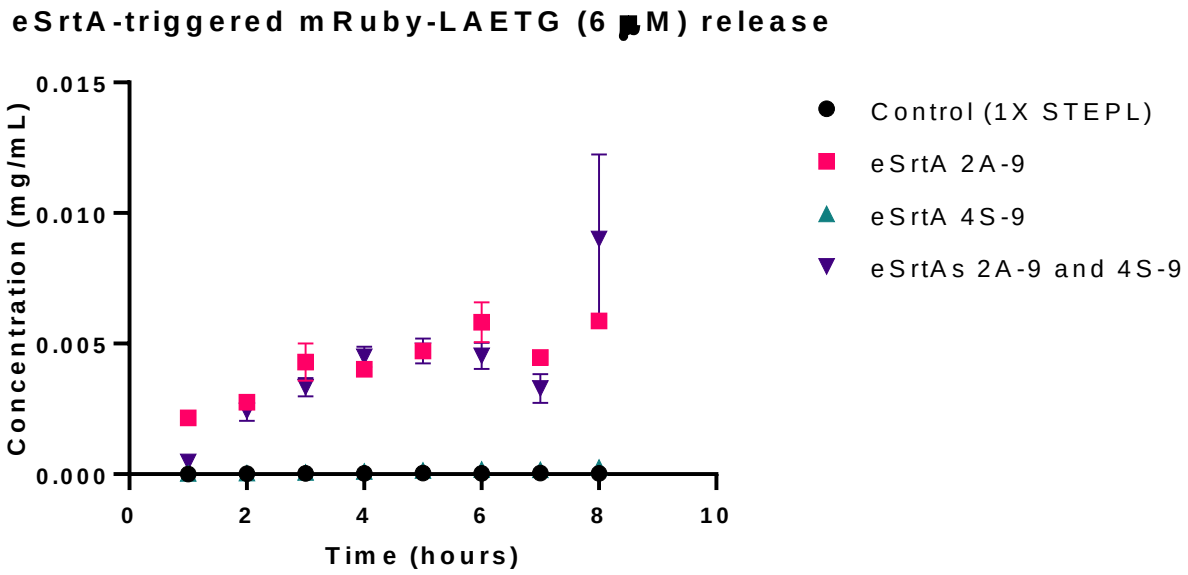

Figure 3.11). Release corresponding to initial tethered [LAETG] is observed to some extent with a comparison of initial mRuby-LAETG concentrations of 3, 6, and 12 μM, with release profiles reflecting relative initial concentrations particularly well between 3 and 6 hours (Figure 3.13). However, again, for a gel with both mRuby-LAETG and mCerulean-LPESG tethered, release profiles for 2A-9, 4S-9, and both 2A-9 and 4S-9 overlap, although sequential release profiles are different from one another, possibly aided by higher initial concentrations before addition of the second sortase (Figure 3.12.)

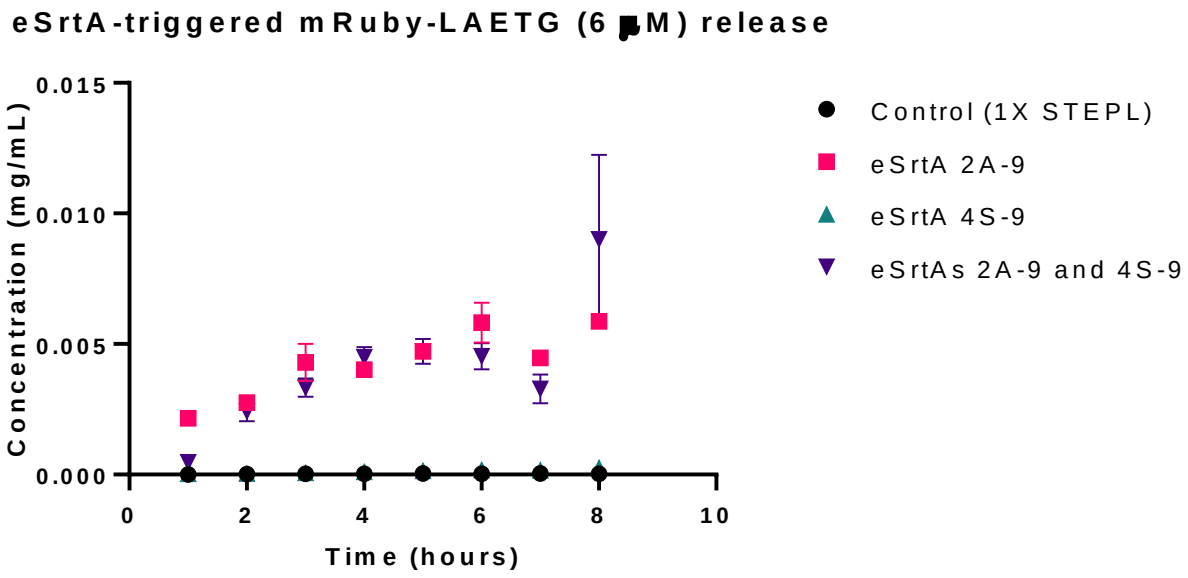

Figure 3.11. Quantification of mRuby-LAETG released into solution over eight hours, with 10 µL mRuby-LAETG-tethered gels, initial mRuby-LAETG concentration of 6 µM, treated with either STEPL buffer (control), eSrtA 2A9, eSrtA 4S9, or both eSrtAs 2A9 and 4S9, in triplicate (error bars denote one standard error of the mean.)

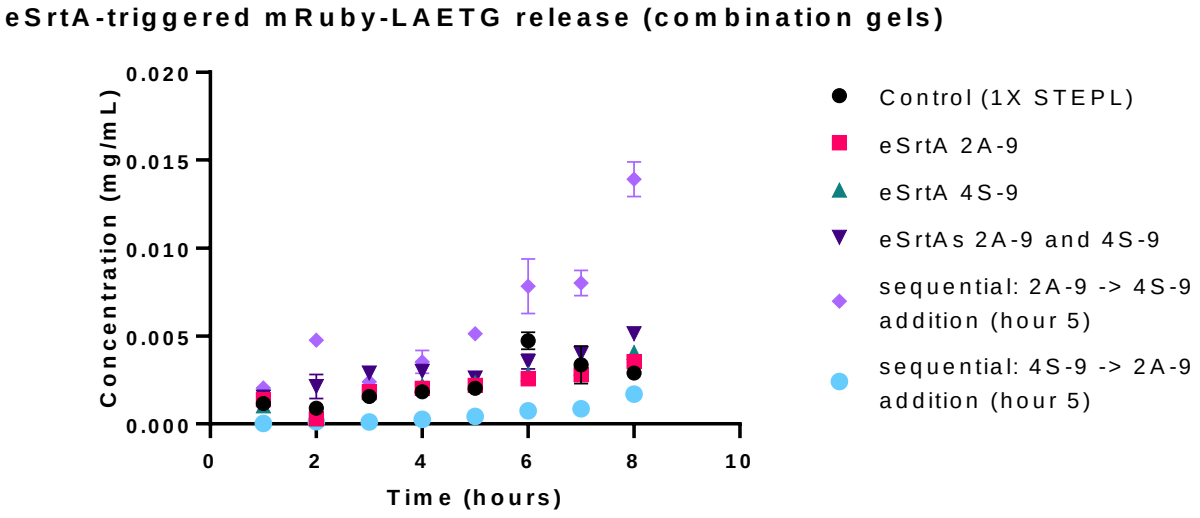

Figure 3.12. Quantification of mRuby-LAETG released into solution over eight hours, with 10 µL mCerulean-LPESG- and mRuby-LAETG-tethered gels, initial tethered protein concentrations of 6 µM, treated with either STEPL buffer (control), eSrtA 2A9, eSrtA 4S9, both eSrtAs 2A9 and 4S9, or with the two eSrtAs in series (2A-9 for 5 hours before 4S-9 addition and vice versa), in triplicate (error bars denote one standard error of the mean.)

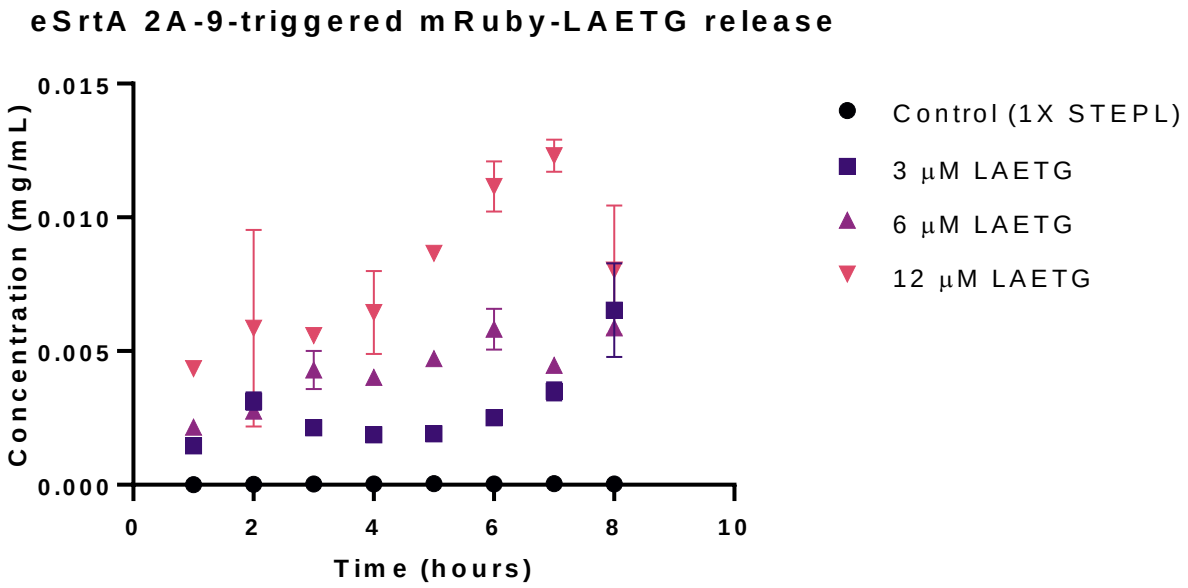

Figure 3.13. Quantification of mRuby-LAETG released into solution over eight hours, with 10 µL mRuby-LAETG-tethered gels, initial tethered protein concentrations of 3, 6, or 9 µM, treated with eSrtA 2A-9, in triplicate (error bars denote one standard error of the mean.)

Chapter 4. CONCLUSIONS

We applied eSrtAs 2A-9 and 4S-9 to selectively release full-length proteins from hydrogel matrices, beyond their initial application to site-specific modification of proteins in aqueous solutions.[35] Additionally, this is a novel demonstration of immobilized site-specifically modified full-length proteins with azide handles, mediated by orthogonal eSrtAs 2A-9 and 4S-9, in PEG-based hydrogels. There is room for potential further optimization of the system to improve upon observed orthogonality of release, e.g., by increasing the relative concentration of eSrtAs with respect to the tethered protein.

As these orthogonal evolved sortases were developed with novel target sequences in mind,[35] more variants of eSrtA could be evolved to selectively act upon other target sequences of interest as substrates with the relatively high catalytic efficiency of prior eSrtA iterations. A similar directed evolution approach could also be applied to increasing the catalytic activity and specificity of alternative sortases with natural orthogonality of activity. This includes the *Streptococcus pyogenes* sortase A, with Ca^{2+}-independent activity towards LPXTA[27], and *Streptomyces avermitilis* sortase E (SavSrtE), which has high Ca^{2+}-independent activity towards the LAXTG motif.[42] Other sortases may similarly be evolved for more efficient activity, such as *S. aureus* sortase B, which uses a NPQTN sorting signal for a different set of natural functions.[24] Beyond sortases, many site-specific proteases exist and mirror evolutionary diversity between species; consequently, many proteases have developed for specificity in a given species and function.[43] This can enable the use of many alternative enzymes, given adequate catalytic efficiency for bioconjugate production or drug release applications.

This work expands the toolkit of orthogonal chemical strategies for modulation of hydrogel properties. A modified short polyglycine probe, which serves as a second substrate in the *Staph. aureus* SrtA mechanism, has recently been used to functionalize biomaterials in a photoactivable manner with growth factors.[44] In combination with orthogonal sortases which also make use of polyglycine as a substrate, this suggests the possibility of using orthogonal sortases and photocleavage groups to improve the range of hydrogel functionality, in highly specific and dynamic terms.

Signaling is tightly controlled in spatial terms and closely connected to the development of complexity in natural systems on many scales. On both the cellular and tissue scale, quantitative and spatial dynamics of signaling receptors play critical roles in development and function.[45] Double-negative feedback appears in morphogen gradients during early development and has also been recapitulated *in vitro*, with potential room for greater control through an extracellular matrix setting.[46] Gradients of signaling molecules are often applied to model developmental processes, such as by forming micropatterned cultures to manipulate spatial availability of a given cytokine[47]; controlling for diffusion across microfluidic devices[48]; or embedding photosensitive cells into long-term brain organoids to monitor network development and functional heterogeneity[49]. The introduction of a biochemically tunable physical matrix for such models can potentially enable another dimension of complexity.[41] Greater control over biological systems is possible as our understanding of natural signaling networks and tissue complexity advances.

BIBLIOGRAPHY

1. Khademhosseini, A., Langer, R., Borenstein, J. & Vacanti, J. P. Microscale technologies for tissue engineering and biology. *Proc. Natl. Acad. Sci.* **103**, 2480–2487 (2006).

2. Lutolf, M. P. & Hubbell, J. A. Synthetic biomaterials as instructive extracellular microenvironments for morphogenesis in tissue engineering. *Nat. Biotechnol.* **23**, 47–55 (2005).

3. Green, J. J. & Elisseeff, J. H. Mimicking biological functionality with polymers for biomedical applications. *Nature* **540**, 386–394 (2016).

4. Madl, C. M., Katz, L. M. & Heilshorn, S. C. Bio-Orthogonally Crosslinked, Engineered Protein Hydrogels with Tunable Mechanics and Biochemistry for Cell Encapsulation. *Adv. Funct. Mater.* **26**, 3612–3620 (2017).

5. Hu, W., Wang, Z. & Xiao, Y. Biomaterials Science Advances in crosslinking strategies of biomedical hydrogels. *Biomater. Sci.* **7**, 843–855 (2019).

6. Sletten, E. M. & Bertozzi, C. R. Bioorthogonal Chemistry: Fishing for Selectivity in a Sea of Functionality. *Angew. Chemie Int. Ed. English* **48**, 6974–6998 (2010).

7. McKay, C. S. & Finn, M. G. Click Chemistry in Complex Mixtures: Bioorthogonal Bioconjugation. *Chem. Biol.* **21**, 1075–1101 (2015).

8. Patterson, D. M., Nazarova, L. A. & Prescher, J. A. Finding the Right (Bioorthogonal) Chemistry. *ACS Chem. Biol.* **9**, 592–605 (2014).

9. Dommerholt, J. & Rutjes, F. P. J. T. Strain-Promoted 1,3-Dipolar Cycloaddition of Cycloalkynes and Organic Azides. *Top. Curr. Chem.* **374**, 1–20 (2016).

10. Agard, N. J., Prescher, J. A. & Bertozzi, C. R. A Strain-Promoted [3 + 2] Azide - Alkyne Cycloaddition for Covalent Modification of Biomolecules in Living Systems. *J. Am. Chem. Soc.* **126**, 15046–15047 (2004).

11. DeForest, C. A., Polizzotti, B. D. & Anseth, K. S. Sequential click reactions for synthesizing and patterning three-dimensional cell microenvironments. *Nat. Mater.* **8**, 659–664 (2009).

12. Fu, S., Dong, H., Deng, X., Zhuo, R. & Zhong, Z. Injectable hyaluronic acid / poly (ethylene glycol) hydrogels crosslinked via strain-promoted azide-alkyne cycloaddition click reaction. *Carbohydr. Polym.* **169**, 332–340 (2017).

13. Lueckgen, A. *et al.* Hydrolytically-degradable click-crosslinked alginate hydrogels. *Biomaterials* **181**, 189–198 (2018).

14. Nimmo, C. M., Owen, S. C. & Shoichet, M. S. Diels - Alder Click Cross-Linked Hyaluronic Acid Hydrogels for Tissue Engineering. *Biomacromolecules* **12**, 824–830 (2011).

15. DeForest, C. A. & Tirrell, D. A. A photoreversible protein-patterning approach for guiding stem cell fate in three-dimensional gels. *Nat. Mater.* **14**, 523–531 (2015).

16. Vianello, S. & Lutolf, M. P. Perspective Understanding the Mechanobiology of Early Mammalian Development through Bioengineered Models. *Dev. Cell* **48**, 751–763 (2019).

17. West, J. L. & Hubbell, J. A. Photopolymerized hydrogel materials for drug delivery applications. *React. Polym.* **25**, 139–147 (1995).

18. Keys, K. B., Andreopoulos, F. M. & Peppas, N. A. Poly(ethylene glycol) Star Polymer Hydrogels. *Macromolecules* **31**, 8149–8156 (1998).

19. Burdick, J. A. & Anseth, K. S. Photoencapsulation of osteoblasts in injectable RGD-modified PEG hydrogels for bone tissue engineering. *Biomaterials* **23**, 4315–4323 (2002).

20. Kloxin, A. M., Kasko, A. M., Salinas, C. N. & Anseth, K. S. Photodegradable Hydrogels for Dynamic Tuning of Physical and Chemical Properties. *Science (80-.).* **324**, 59–64 (2009).

21. Mosiewicz, K. A. *et al.* In situ cell manipulation through enzymatic hydrogel photopatterning. *Nat. Mater.* **12**, 1072–1078 (2013).

22. Deiss, F., Mazzeo, A., Hong, E., Ingber, D. E. & Derda, R. Platform for High-Throughput Testing of the E ff ect of Soluble Compounds on 3D Cell Cultures. *Anal. Chem.* **85**, 8085 (2013).

23. Clancy, K. W., Melvin, J. A. & McCafferty, D. G. Sortase Transpeptidases: Insights into Mechanism, Substrate Specificity and Inhibition. *Biopolymers* **94**, 385–396 (2010).

24. Jacobitz, A. W. *et al.* Structural and Computational Studies of the Staphylococcus aureus Sortase B-Substrate Complex Reveal a Substrate-stabilized Oxyanion Hole. *J. Biol. Chem.* **289**, 8891–8902 (2014).

25. Ham, H. O. *et al.* In situ regeneration of bioactive coatings enabled by an evolved Staphylococcus aureus sortase A. *Nat. Commun.* **7**, 11140 (2016).

26. Wang, X., Chen, J., Otting, G. & Su, X. Conversion of an amide to a high- energy thioester by Staphylococcus aureus sortase A is powered by variable binding affinity for calcium. *Sci. Rep.* **8**, 2–10 (2018).

27. Guimaraes, C. P. *et al.* Site-specific C-terminal and internal loop labeling of proteins using sortase-mediated reactions. *Nat. Protoc.* **8**, 1787 (2013).

28. Warden-Rothman, R., Caturegli, I., Popik, V. & Tsourkas, A. Sortase-Tag Expressed Protein Ligation: Combining Protein Purification and Site-Specific Bioconjugation into a Single Step. *Anal. Chem.* **85**, 11090–11097 (2013).

29. Popp, M. W., Antos, J. M., Grotenbreg, G. M., Spooner, E. & Ploegh, H. L. Sortagging: a versatile method for protein labeling. *Nat. Chem. Biol.* **3**, 707–708 (2007).

30. Shadish, J. A., Benuska, G. M. & DeForest, C. A. 4D patterning of gel biomaterials. *Nat. Mater.* (2019). doi:10.1038/s41563-019-0367-7

31. Cambria, E. *et al.* Covalent Modification of Synthetic Hydrogels with Bioactive Proteins via Sortase-Mediated Ligation. *Biomacromolecules* **16**, 2316–2326 (2015).

32. Gau, E. *et al.* Sortase-Mediated Surface Functionalization of Stimuli-Responsive Microgels. *Biomacromolecules* **18**, 2789–2798 (2017).

33. Moore, D. M. Dynamic Control of Hydrogel Properties via Enzymatic Reactions. (Indiana University-Purdue University Indianapolis (IUPUI), 2019).

34. Arkenberg, M. R., Moore, D. M. & Lin, C. Dynamic control of hydrogel crosslinking via sortase-mediated reversible transpeptidation. *Acta Biomater.* **83**, 83–95 (2019).

35. Dorr, B. M., Ham, H. O., An, C., Chaikof, E. L. & Liu, D. R. Reprogramming the specificity of sortase enzymes. *Proc. Natl. Acad. Sci.* **111**, 13343 LP – 13348 (2014).

36. Antos, J. M., Truttmann, M. C. & Ploegh, H. L. Recent Advances in Sortase-Catalyzed Ligation Methodology. 111–118 (2017). doi:10.1016/j.sbi.2016.05.021.Recent

37. Chen, I., Dorr, B. M. & Liu, D. R. A general strategy for the evolution of bond-forming enzymes using yeast display. *Proc. Natl. Acad. Sci.* **108**, 11399–11404 (2011).

38. Bretherton, R. *Unpublished*. (2020).

39. Aguado, B. A., Grim, J. C., Rosales, A. M., Watson-capps, J. J. & Anseth, K. S. Engineering precision biomaterials for personalized medicine. *Sci. Transl. Med.* **10**, (2018).

40. Raman, R. *et al.* Light-degradable hydrogels as dynamic triggers for gastrointestinal applications. *Sci. Adv.* **6**, 1–11 (2020).

41. Zhu, X. *et al.* Directing three-dimensional multicellular morphogenesis by self-organization of vascular mesenchymal cells in hyaluronic acid hydrogels. *J. Biol. Eng.* **11**, 1–12 (2017).

42. Das, S. *et al.* Structure and specificity of a new class of Ca 2+-independent housekeeping sortase from Streptomyces avermitilis provide insights into its non-canonical substrate preference. *J. Biol. Chem.* **292**, 7244–7257 (2017).

43. Lopez-Otin, C. & Bond, J. S. Proteases : Multifunctional Enzymes in Life and Disease. *J. Biol. Chem.* **283**, 30433–30437 (2008).

44. Broguiere, N. *et al.* Morphogenesis Guided by 3D Patterning of Growth Factors in Biological Matrices. *Adv. Mater.* **1908299**, 1–10 (2020).

45. Casaletto, J. B. & McClatchey, A. I. Spatial regulation of receptor tyrosine kinases in development and cancer. *Nat. Rev. Cancer* **12**, 387–400 (2012).

46. Li, P. *et al.* Morphogen gradient reconstitution reveals Hedgehog pathway design principles. *Science (80-.).* **360**, 543–548 (2018).

47. Warmflash, A., Sorre, B., Etoc, F., Siggia, E. D. & Brivanlou, A. H. A method to recapitulate early embryonic spatial patterning in human embryonic stem cells. *Nat. Methods* **11**, 847–854 (2014).

48. Manfrin, A. *et al.* Engineered signaling centers for the spatially controlled patterning of human pluripotent stem cells. *Nat. Methods* **16**, 640–648 (2019).

49. Quadrato, G. *et al.* Cell diversity and network dynamics in photosensitive human brain organoids. *Nature* **545**, 48–53 (2017).